SANDIA REPORT
SAND2014-17460
Unlimited Release
Printed September 2014

Wave Energy Converter Effects on Wave Fields: Evaluation of SNL-SWAN and Sensitivity Studies in Monterey Bay, CA

Grace Chang, Jason Magalen, Craig Jones, Jesse Roberts

Prepared by
Sandia National Laboratories
Albuquerque, New Mexico 87185 and Livermore, California 94550

Sandia National Laboratories is a multi-program laboratory managed and operated by Sandia Corporation, a wholly owned subsidiary of Lockheed Martin Corporation, for the U.S. Department of Energy's National Nuclear Security Administration under contract DE-AC04-94AL85000.

Issued by Sandia National Laboratories, operated for the United States Department of Energy by Sandia Corporation.

Available to DOE and DOE contractors from
U.S. Department of Energy
Office of Scientific and Technical Information
P.O. Box 62
Oak Ridge, TN 37831

Telephone: (865) 576-8401
Facsimile: (865) 576-5728
E-Mail: reports@adonis.osti.gov
Online ordering: http://www.osti.gov/bridge

Available to the public from
U.S. Department of Commerce
National Technical Information Service
5285 Port Royal Rd.
Springfield, VA 22161

Telephone: (800) 553-6847
Facsimile: (703) 605-6900
E-Mail: orders@ntis.fedworld.gov
Online order: http://www.ntis.gov/help/ordermethods.asp?loc=7-4-0#online

SAND2014-17460
Unlimited Release
Printed September 2014

Wave Energy Converter Effects on Wave Fields: Evaluation of SNL-SWAN and Sensitivity Studies in Monterey Ba, CA

Grace Chang, Jason Magalen, and Craig Jones
Sea Engineering, Inc.
200 Washington Street, Suite 101
Santa Cruz, CA 95060

Jesse Roberts
Water Power
Sandia National Laboratories
P.O. Box 5800
Albuquerque, New Mexico 87185-MS1124

Abstract

A modified version of an industry standard wave modeling tool was evaluated, optimized, and utilized to investigate model sensitivity to input parameters and wave energy converter (WEC) array deployment scenarios. Wave propagation was investigated downstream of the WECs to evaluate overall near- and far-field effects of WEC arrays. The sensitivity study illustrated that wave direction and WEC device type were most sensitive to the variation in the model parameters examined in this study. Generally, the changes in wave height were the primary alteration caused by the presence of a WEC array. Specifically, WEC device type and subsequently their size directly resulted in wave height variations; however, it is important to utilize ongoing laboratory studies and future field tests to determine the most appropriate power matrix values for a particular WEC device and configuration in order to improve modeling results.

ACKNOWLEDGMENTS

The research and development described in this document was funded by the U.S. Department of Energy. Sandia is a multiprogram laboratory operated by Sandia Corporation, a Lockheed Martin Company, for the United States Department of Energy's National Nuclear Security Administration under contract DE-AC04-94AL85000.

This research was made possible by support from the Department of Energy's Wind and Water Power Technologies Office.

CONTENTS

FIGURES

TABLES

NOMENCLATURE

CCW	Counter clockwise
B-HBA	Bottom-fixed heave-buoy array
B-OF	Bottom-fixed oscillating flap
Bref-HB	Small bottom-referenced heaving buoy
Bref-SHB	Bottom-referenced submerged heave-buoy
CDIP	Coastal Data Information Program
CW	Clockwise
DOE	Department of Energy
dd	Directional spreading coefficient
F-2HB	Floating two-body heaving converter
F3 OF	Floating three-body oscillating flap device
F-HBA	Floating heave-buoy array
F-OWC	Floating oscillating water column
H_s	Significant wave height
Kt	Transmission coefficient
Ktp	1 – RCW
mdc	Directional resolution
MWD	Mean wave direction
NDBC	National Data Buoy Center
NOAA	National Oceanic and Atmospheric Administration
NWW3	WaveWatch III
PTO	Power take-off
RCW	Relative capture width
SNL	Sandia National Laboratories
SWAN	Simulating WAves Nearshore
SNL-SWAN	Modified SWAN model
T_p or T_s	Peak wave period
WEC	Wave energy converter

1. INTRODUCTION

In order to effectively convert wave energy into commercial-scale onshore electrical power, wave energy converter (WEC) devices need to be installed in arrays comprising multiple devices. The deployment of WEC arrays will begin small (pilot-scale or ~10 devices) but could feasibly number in the hundreds of individual devices at commercial-scale. As the industry progresses from pilot- to commercial-scale it is important to understand and quantify the effects of WECs on the natural nearshore processes that support a local, healthy ecosystem. WEC arrays have the potential to alter nearshore wave propagation and circulation patterns, possibly modifying sediment transport patterns and ecosystem processes. As WEC arrays sizes grow, there is a potential for negative environmental impacts which could be detrimental to local coastal ecology, and social and economic services. To help accelerate the realization of commercial-scale wave power, predictive modeling tools have been developed and utilized to investigate ranges of anticipated scenarios to evaluate the potential for negative (or positive) environmental impact.

At present, direct measurements of the effects of different types of WEC arrays on wave properties for a prototype scale WEC site are not available; therefore, the effects of varying WEC types and model parameters on model results must be evaluated before environmental assessments can be completed. Wave model simulations provide the groundwork for completing such assessments by investigating the sensitivity of the predictive model results to prescribed model parameters and WEC characteristics over a range of anticipated wave conditions. The understanding developed here will allow investigators to conduct predictive environmental assessments with increased confidence and reduced uncertainty in future phases.

The present study incorporates a modified version of an industry standard wave modeling tool, SWAN (Simulating WAves Nearshore), to simulate wave propagation through a hypothetical WEC array deployment site on the California coast. The modified SWAN, referred to as SNL-SWAN, attempts to incorporate device-specific WEC power take-off (PTO) characteristics to more accurately evaluate a WEC device's effects on wave propagation and ultimately nearshore hydrodynamics.

1.1. Objectives

The primary objectives of the SNL-SWAN evaluation and WEC sensitivity study were to evaluate SNL-SWAN in comparison to the native SWAN code and to investigate the effects of a range of WEC devices on nearshore wave propagation using SNL-SWAN model simulations. To accomplish this, the following tasks were undertaken:

(1) Evaluate the modified wave propagation model, SNL-SWAN, which allows the incorporation of device-specific WEC characteristics to assess their effects on nearshore wave propagation.
(2) Optimize SNL-SWAN model parameters to minimize model artifacts and edge effects.
(3) Perform model sensitivity analysis using SNL-SWAN to further examine the effects of model variations (incident wave height, period, frequency distribution spread, directional

distribution spread, WEC device type and size, number of WECs, and WEC device spacing within the WEC array) on near-field and far-field wave conditions in the lee of the WEC devices, in a manner similar to that employed on the native SWAN model (Chang et al., 2014).

(4) Investigate the differences in derived transmission coefficients for SNL-SWAN switch 1 and switch 2 ("switches" are described below).

2. SNL-SWAN MODEL EVALUATION

The modified wave model, SNL-SWAN, attempts to incorporate device-specific WEC PTO characteristics to more accurately evaluate each device's effects on wave propagation and ultimately nearshore hydrodynamics. SNL-SWAN calculates the relative capture width (RCW) or ratio of incident wave power to captured wave power by a specific WEC device given the initial wave conditions (e.g., wave height, H_s, and period, T_p). The RCW value is then returned to the SWAN program and is used for calculation of the transmission coefficient, Kt, for the WEC device, which is specified as an obstacle in SWAN, where: Kt = sqrt(Ktp) and Ktp = 1 – RCW. Three methods of determining the transmission coefficient are employed in SNL-SWAN, hereafter referred to as "switch 0", "switch 1" and "switch 2", respectively:

0) SNL-SWAN defers to the native SWAN code, i.e. the transmission coefficient is user-specified in the INPUT file,
1) SNL-SWAN computes the RCW from a user-supplied device-specific power matrix (e.g., Table 1 shows an example power matrix for a particular device), or
2) The user supplies the RCW for a specific wave height and period, where
   RCW = Power Matrix Value / Incident Power / Device Width and
   Incident Power = $0.42 * H_s^2 * T_p$.

The power matrices for a variety of existing WEC devices were computed based on the numerical approach described by Babarit et al. (2012).

Table 1. Power matrix computed for a floating two-body heaving converter.

		Tp														
	MEAN	3	4	5	6	7	8	9	10	11	12	13	14	15	16	17
Hs (m)	0.5	0.60	1.61	2.64	4.89	6.39	8.37	12.67	13.67	11.61	10.11	9.24	6.38	4.58	3.80	3.55
	1	2.38	6.17	11.41	18.98	24.59	30.05	43.58	50.23	53.08	43.89	34.42	21.92	19.86	16.76	11.78
	1.5	0.00	13.28	24.89	43.33	55.25	67.96	90.01	102.02	92.00	90.80	66.10	64.76	44.93	37.35	21.63
	2	0.00	24.41	45.28	65.12	100.01	120.52	153.17	174.68	150.81	121.65	126.08	86.91	60.69	58.10	48.03
	2.5	0.00	0.00	65.28	104.49	140.87	190.70	179.31	242.52	254.65	189.64	180.67	134.90	99.21	83.45	81.33
	3	0.00	0.00	96.17	136.56	204.65	243.52	357.25	293.48	352.72	259.94	248.15	184.35	136.67	119.64	112.52
	3.5	0.00	0.00	125.80	191.86	253.97	291.27	431.21	385.28	424.16	314.11	285.14	238.78	221.66	172.20	126.00
	4	0.00	0.00	0.00	256.49	366.25	403.22	550.98	536.25	530.82	472.85	419.89	288.55	268.44	178.63	193.75
	4.5	0.00	0.00	0.00	326.93	418.27	574.17	677.66	707.97	664.65	509.15	415.11	385.96	243.88	249.11	200.10
	5	0.00	0.00	0.00	358.22	514.29	658.21	824.37	827.96	617.58	638.26	512.41	451.81	384.04	332.79	257.61
	5.5	0.00	0.00	0.00	448.06	609.99	773.94	879.67	935.80	904.97	804.91	602.74	456.08	396.61	310.94	308.35
	6	0.00	0.00	0.00	0.00	710.80	952.47	973.55	1000.00	838.26	886.05	648.39	500.95	502.78	396.33	388.41
	6.5	0.00	0.00	0.00	0.00	788.43	1000.00	1000.00	1000.00	978.75	1000.00	726.81	577.45	435.21	423.53	357.60
	7	0.00	0.00	0.00	0.00	781.16	1000.00	1000.00	1000.00	1000.00	1000.00	959.05	748.36	573.85	471.83	449.84
	7.5	0.00	0.00	0.00	0.00	993.77	1000.00	1000.00	1000.00	1000.00	1000.00	1000.00	754.57	724.83	641.66	482.11

2.1. SNL-SWAN Evaluation Model Set-Up

For simplicity, the SNL-SWAN model evaluation was conducted using a two-nested model domain (Monterey Bay and Santa Cruz) with the same model set-up as described in Chang et al. (2014) (Figure 1). A previously validated SWAN model for the same region was used to propagate waves from deep-water offshore to shallow water. Several local National Oceanic and Atmospheric Administration National Data Buoy Center (NOAA NDBC) buoys provided measurements of significant wave heights, dominant wave periods, peak wave directions, wind speeds and wind directions at the buoy locations dating as far back as 1987. These measured

datasets were compared to model output to demonstrate excellent model performance. The wave model and validation were discussed in Chang et al. (2010, unpublished).

Two SNL-SWAN model grids were nested to predict the propagation of deep-water waves from offshore of Monterey Bay, CA, to nearshore Santa Cruz, CA. The Monterey Bay and Santa Cruz model domains are shown in Figure 1. The coarse-grid (herein referred to as the Monterey Bay model domain) resolution was approximately 0.001° degrees in latitude and longitude (approximately 100 m grid spacing in x and y). The model was run as a stationary model: meteorological and hydrodynamic conditions at the offshore boundaries were kept constant. Directional wave energy spectra conditions were exported from the coarse resolution model and used as boundary conditions for the nested, fine resolution model (herein referred to as the Santa Cruz model domain).

The grid resolution of the nested Santa Cruz model domain computational grid was matched to the size of the modeled WEC device type. For SNL-SWAN model evaluation, the device size and type chosen was a 25-m floating two-body heaving converter (F-2HB; Babarit, 2012). The Santa Cruz model grid size was therefore approximately 0.00025° degrees in latitude and longitude. The wave spectrum boundary conditions were applied along the offshore boundaries of the Santa Cruz SNL-SWAN model domain. The nested grid model was also implemented as a stationary model.

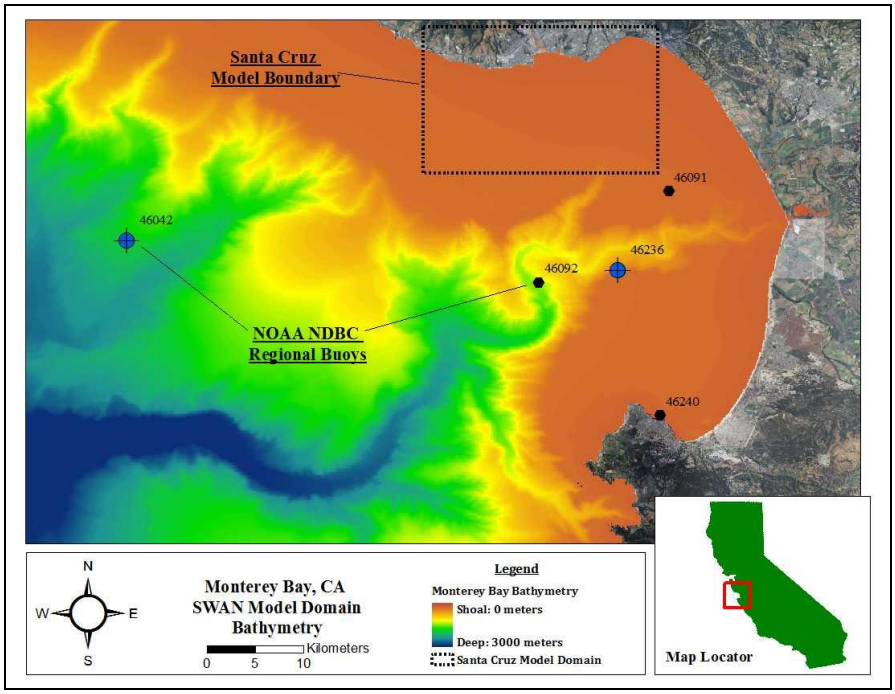

Figure 1. Monterey Bay and Santa Cruz, CA model domains used for SNL-SWAN model evaluation.

SNL-SWAN was operated for three different cases: (0) Switch 0, (1) Switch 1 and (2) Switch 2 and the native SWAN model was also utilized for comparison. The initial wave conditions were: 1.5 m significant wave height, 12.5 s wave peak (?) period, 205° mean wave direction, frequency distribution spread of 3.3, and directional distribution spread of 10.

All four model runs (three SNL-SWAN switches and one native SWAN model run) incorporated an array of 10 WEC devices with zero wave energy reflection allowed, centered on the 40 m depth contour. The WEC device array was arranged in a honeycomb/diamond-shape as a representative configuration (Figure 2). WEC devices were simulated in the model with 6-diameter spacing between devices, center to center. Devices were equally spaced in all directions. Again, the simulated WEC device type was a floating two-body heaving converter with 25 m diameter (same as the grid spacing for the nested Santa Cruz model domain).

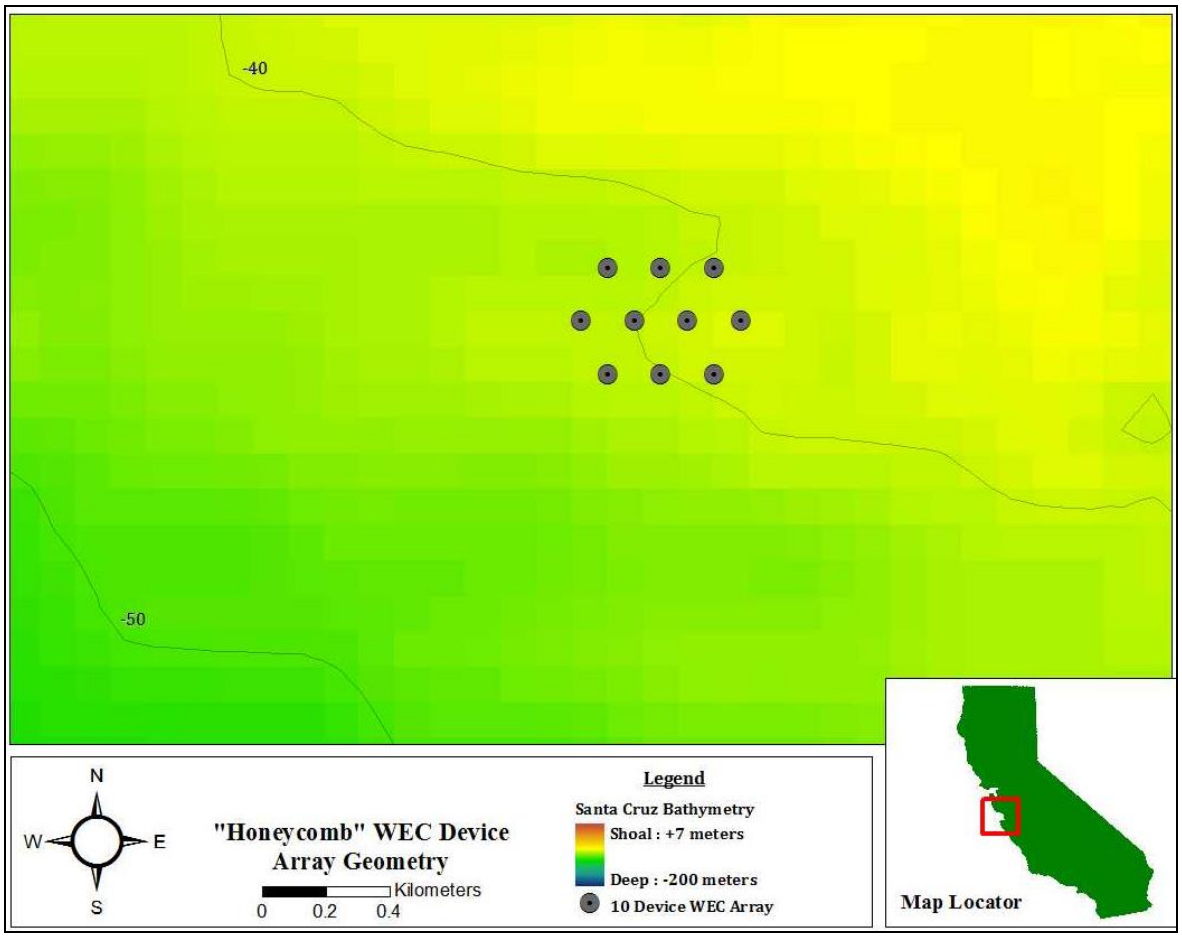

Figure 2. Example honeycomb geometry of a 10-WEC device array in the model.

The model results were evaluated at six shoreline locations along the Santa Cruz coast on the 10 m, 20 m, and 30 m depth contours as described in

Table 2 and shown in Figure 3. The shoreline locations were, from west to east:

- West Santa Cruz
- Steamer Lane
- Santa Cruz Wharf
- Santa Cruz Harbor
- East 26th Ave.
- Pleasure Point

Table 2. Model output locations for SNL-SWAN model evaluation.

Output Location Number	Depth Contour and Description	Output Location Number	Depth Contour and Description
1	30 m - West Santa Cruz	10	30 m – Santa Cruz Harbor
2	20 m - West Santa Cruz	11	20 m – Santa Cruz Harbor
3	10 m - West Santa Cruz	12	10 m – Santa Cruz Harbor
4	30 m - Steamer Lane	13	30 m – East 26th Ave
5	20 m - Steamer Lane	14	20 m – East 26th Ave
6	10 m - Steamer Lane	15	10 m – East 26th Ave
7	30 m – Santa Cruz Wharf	16	30 m - Pleasure Point
8	20 m – Santa Cruz Wharf	17	20 m - Pleasure Point
9	10 m – Santa Cruz Wharf	18	10 m - Pleasure Point

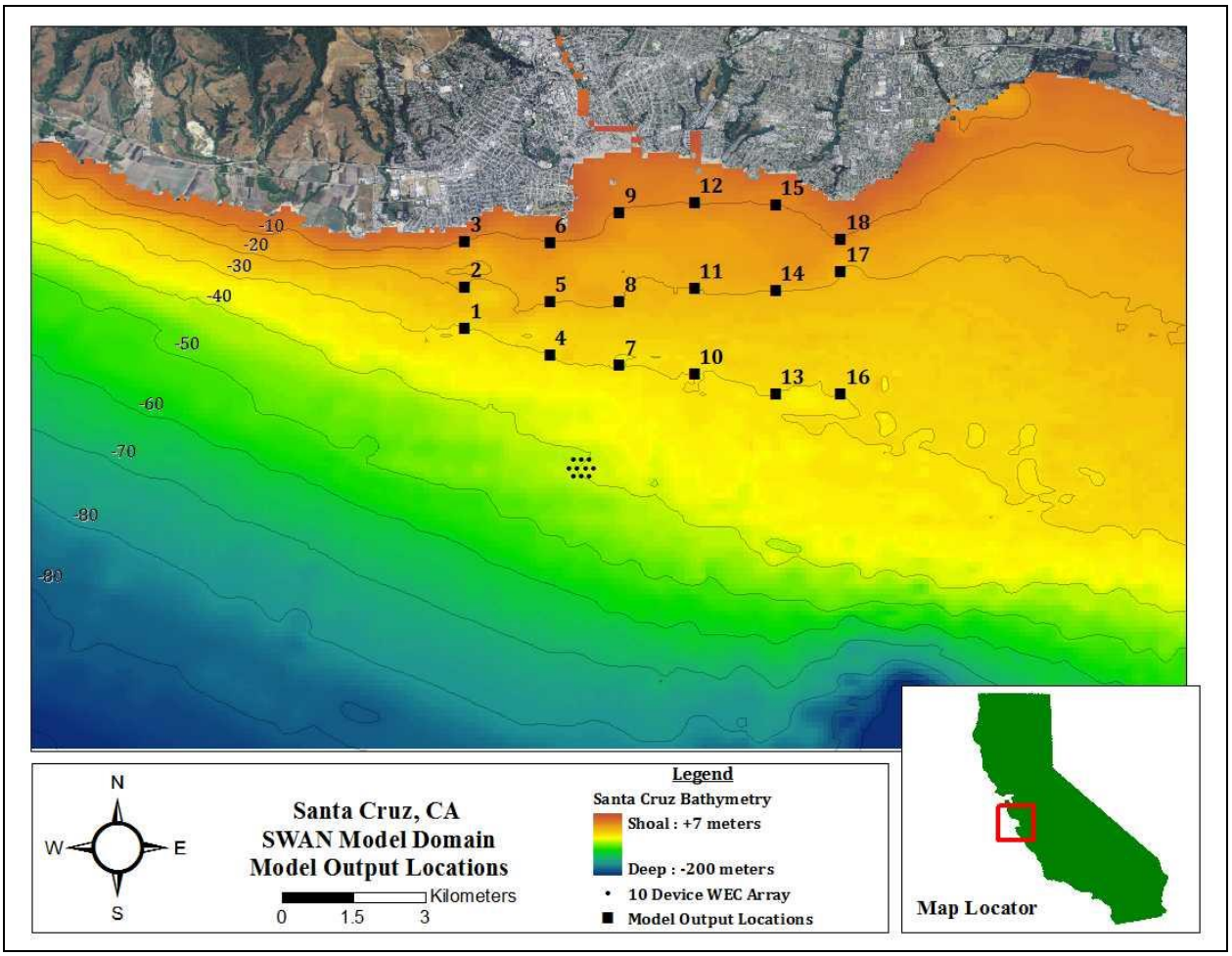

Figure 3. Eighteen model output locations in the Santa Cruz, CA model domain with example WEC device array shown.

2.2. SNL-SWAN Evaluation Results

SNL-SWAN was first run for Switch 2 and then for Switch 1. The computed transmission coefficient (Kt) outputs for the 10 WEC array from the Switch 2 and Switch 1 model runs nearly identical (

Table 3). Thus, the average Kt value of 0.86 was specified as the transmission coefficient for SNL-SWAN Switch 0 and for the native SWAN model run. Results were evaluated for the 18 output locations as described above.

SNL-SWAN Switch 0 and native SWAN runs with the transmission coefficient specified as 0.86 yielded identical results (Figure 4). Results from SNL-SWAN Switch 1 and Switch 2 were nearly identical to each other (only one output location, 7, differed by 0.1 cm) and to SNL-SWAN Switch 0 and native SWAN results. The maximum difference in simulated wave height between SNL-SWAN Switch 1 and Switch 2 compared to SNL-SWAN Switch 0 and native SWAN was 0.5 cm at the locations directly in the lee of the WECs. These results indicate that

the SNL-SWAN wave model was generally operating as intended, at least for the conditions specified here for SNL-SWAN model evaluation.

Table 3. Transmission coefficients (Kt) for 10 WEC devices computed from SNL-SWAN evaluation model runs, Switch 1 and Switch 2.

	Kt									
Switch #	**WEC 1**	**WEC 2**	**WEC 3**	**WEC 4**	**WEC 5**	**WEC 6**	**WEC 7**	**WEC 8**	**WEC 9**	**WEC 10**
1	0.856	0.854	0.854	0.856	0.855	0.855	0.856	0.856	0.856	0.857
2	0.860	0.860	0.860	0.860	0.860	0.860	0.860	0.860	0.860	0.860

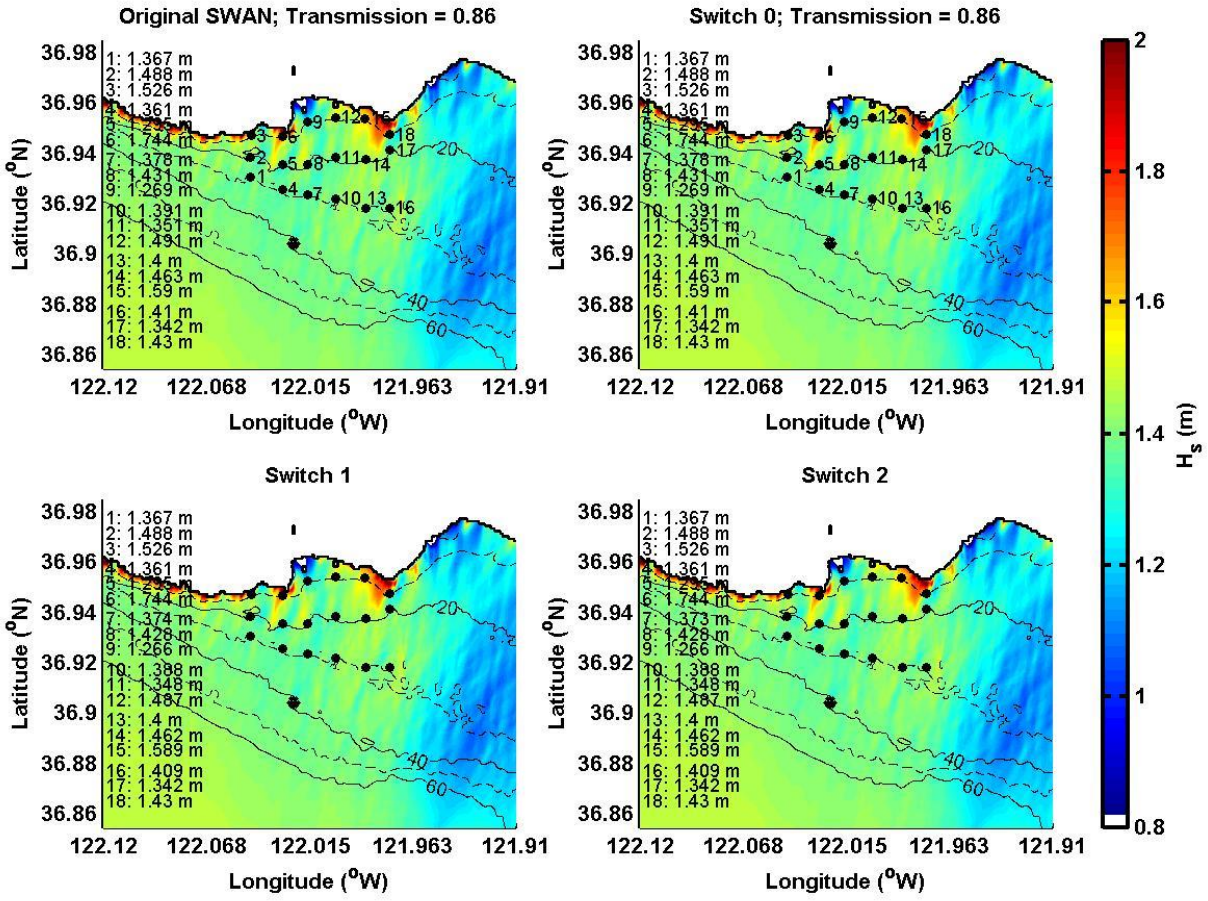

Figure 4. Simulated wave height for SNL-SWAN model evaluation runs. The text on the left indicates the simulated wave height at each of the 18 output locations.

3. SNL-SWAN MODEL PARAMETER OPTIMIZATION

A series of SNL-SWAN model runs were performed while varying directional resolution (model parameter 'mdc') as well as the directional spreading coefficient ('dd') in order to minimize model numerical artifacts. The effects of diffraction were also investigated in the model parameter optimization runs.

3.1. SNL-SWAN Optimization Model Set-Up

Similar to the SNL-SWAN model evaluation runs, the selected modeling site was nearshore Monterey Bay and Santa Cruz, California (Figure 1). Two SNL-SWAN model grids were nested to predict the propagation of deep-water waves from offshore of Monterey Bay, CA, to near-shore Santa Cruz, CA. The Monterey Bay model domain resolution was approximately 0.001° degrees in latitude and longitude and the grid resolution of the nested Santa Cruz model domain computational grid was matched to the size of the modeled WEC device type. For model optimization runs, the device size and type chosen was a 20-m floating two-body heaving converter (F-2HB; Babarit, 2012).

Historical wave conditions offshore of Monterey Bay are fairly well understood due to the existence of long-term wave data measurements from several NOAA NDBC and Coastal Data Information Program (CDIP) buoys. Representative data from NOAA NDBC buoy #46042 were utilized to determine typical wave conditions to be expected in the Monterey Bay region. The buoy is located 27 nautical miles west-northwest of Monterey, CA, in greater than 2000 meters water depth. Data have been recorded at this location since 1987, making it a statistically reliable source for evaluating typical (and extreme) wave conditions approaching Monterey Bay.

A wave height and wave period rose was generated by the historical data to evaluate the historical wave climate.[1] Significant wave height is the average of the highest 1/3 of wave heights on record. Dominant wave periods correspond directly to the frequency containing the largest amount of wave energy. Mean wave directions are the directions *from* which the dominant waves (waves corresponding to the dominant period) are approaching.

Figure 5 illustrates that the dominant wave direction (most frequently occurring) was from the northwesterly direction. The plots also indicate the most frequently occurring wave heights and wave periods (magnitude of color bands in plots). The basic statistics (of all available wave data from this buoy) that resulted from the wave data analysis are listed in Table 4. Figure 6, Figure 7, and Figure 8 show the statistical histograms of each wave property and provide a visual comparison to the model input values selected for the present modeling effort. It is evident that the majority of the waves approach the Monterey Bay region from the northwest (270 – 360 degrees True North) and that more than half of the waves on record are comprised of wave heights of 2.0 meters or less and wave periods of less than 12 seconds.

[1]Wave heights are the significant wave heights; the wave periods are the dominant wave periods. The wave directions are the mean wave direction, MWD, recorded by the buoy, and are the directions *from* which the waves approach.

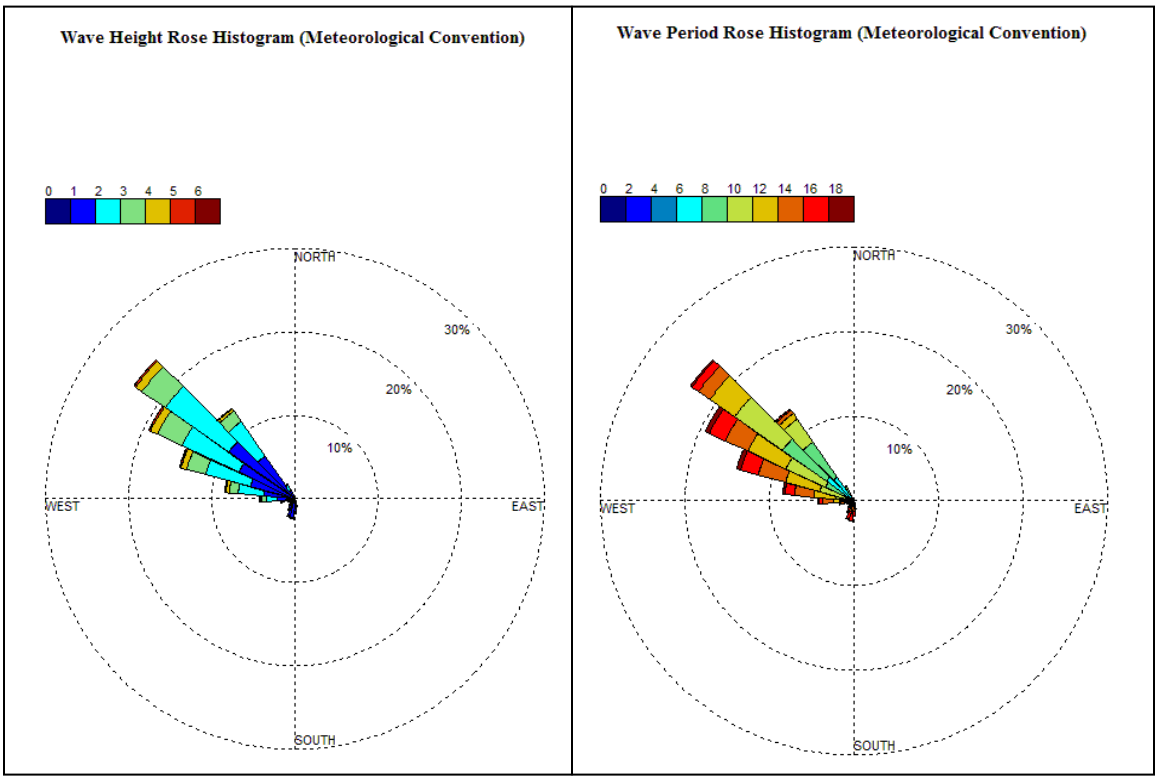

Figure 5. Wave height (left) and wave period (right) rose diagrams showing direction *from* which the waves are approaching. Data collected by NOAA NDBC buoy #46042.

Table 4. Statistical data analysis - NOAA NDBC buoy #46042.

Parameter and Units	Mean Value	Median Value	Mode Value
H_s (m)	2.2	2.0	1.7
T_p (s)	11.8	11.4	12.5
MWD (degrees)	287.5	299	310

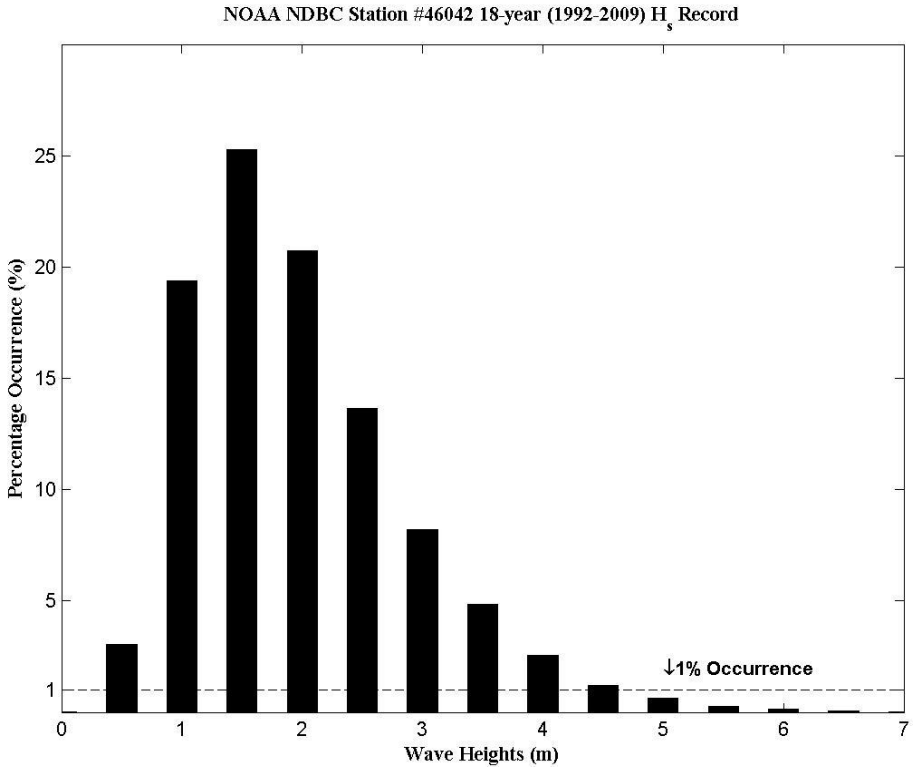

Figure 6. Wave height histogram (frequency of occurrence) - NOAA NDBC buoy #46042.

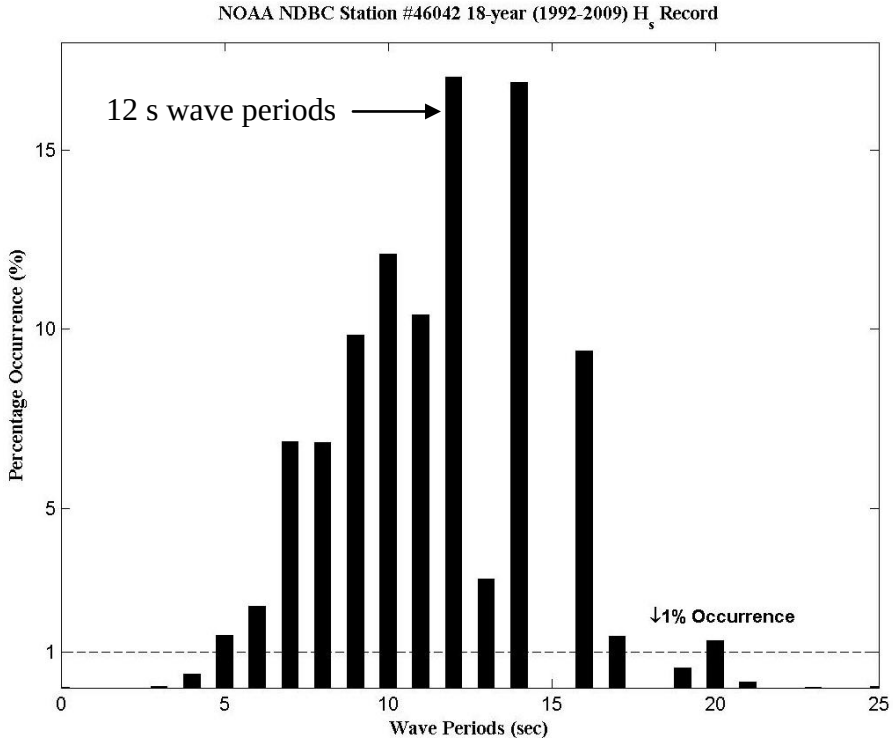

Figure 7. Wave period histogram (frequency of occurrence) - NOAA NDBC buoy #46042.

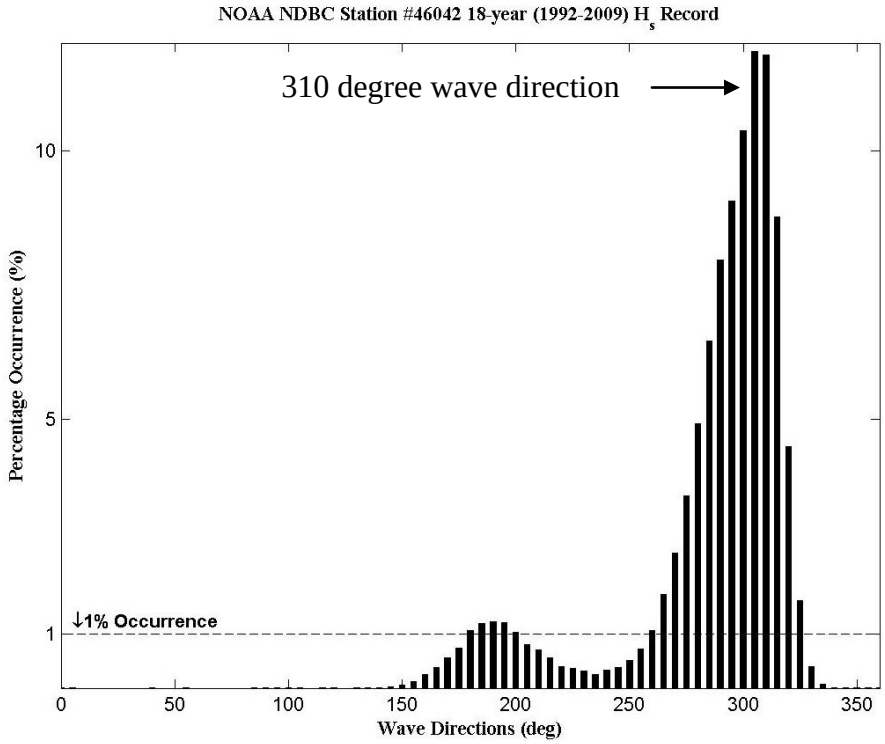

Figure 8. Wave direction histogram (frequency of occurrence) - NOAA NDBC buoy #46042.

In order to model a scenario with potential nearshore (and shoreline) Santa Cruz impacts, representative offshore wave conditions were selected based on their potential to alter nearshore wave properties. Based on the data analyzed from NOAA NDBC buoy #46042, H_s = 1.7 m, T_p = 12.5 sec was selected for representative offshore boundary conditions (Table 5). The offshore mean wave directions applied at the boundaries were 310 degrees and 205 degrees (Table 5), chosen because these caused wave shadowing to occur in the direction of the nearest shoreline (distance of order 5 km) to the simulated WEC deployment locations.

Table 5. Model Boundary Conditions.

Parameter (units)	Values
H_s (m)	1.7
T_p (sec)	12.5
MWD (degrees)	205

This was a conservative approach at modeling WEC array impacts on nearshore wave properties because waves approach Santa Cruz from a southwesterly direction (180° to 270° True North) approximately 15% of the time and waves approach the region from a northwesterly direction

(270° to 360° True North) approximately 80% of the time. These simulations, however, illustrated the potential effects on wave properties near the Santa Cruz shoreline if a WEC array were to be installed in locations offshore of Santa Cruz.

Offshore model boundary conditions were specified for all "wet" boundaries (north, west and south sides) of the Monterey Bay domain. Waves were propagated from offshore to onshore throughout the entire domain. Wave frequency and directional spectra were extracted along the "wet" boundaries of the Santa Cruz domain and used as input boundary conditions for the nested, Santa Cruz domain (**Error! Reference source not found.**). Waves were then propagated from the offshore boundaries of the Santa Cruz model domain to the shoreline.

In the present analysis, the WEC device was the 20-m F-2HB buoy type, chosen because of its relatively large size and hence its simplicity in equating its diameter to the model computational grid size. An array of 50 WEC devices spaced six diameters apart on the 40 m depth contour was modeled. The WEC device array was arranged in a honeycomb/diamond-shape as a representative configuration (Figure 2). WEC devices were simulated in the model parameter optimization study with 6-diameter spacing between devices, center to center. Devices were equally spaced in all directions. Model output location information is described above and shown in Table 2 and Figure 3.

3.2. SNL-SWAN Model Optimization Parameters

Based on the data analyzed from NOAA NDBC buoy #46042, the mode of the wave heights and periods, 1.7 m and 12.5 sec, respectively, were selected for the incident wave height and wave period conditions. Gamma (frequency spreading coefficient) was held constant at 3.3.

Directional resolution was varied between 15° and 9° ('mdc' equal to 24 and 40, respectively); 9° was the highest angular resolution possible with the smallest desired computational grid size of 5 m (directional resolution greater than 9° resulted in model allocation errors). The two different 'mdc' values of 24 and 40 were run with directional spread (model parameter 'dd') varying between 10 and 25 and diffraction turned on and off. Diffraction settings, when turned on, followed SWAN recommended smoothing parameters (a = 0.2 and n = 6). A total of eight (8) model parameter optimization runs were performed, as indicated in Table 6. Results were compared to model runs performed with the same parameter values but with no WEC devices, where percent difference was computed following:

$$Percentage\ Change = \frac{(InitialValue - FinalValue)}{InitialValue} \times 100 \qquad \text{Eq. 1}$$

where InitialValue and FinalValue was H_s determined from model runs without WEC devices and with WEC devices, respectively.

Table 6. SNL-SWAN model parameter optimization scenarios

Run	mdc	dd	DIFFRaction
1	24	10	OFF
2	24	10	ON
3	24	25	OFF
4	24	25	ON
5	40	10	OFF
6	40	10	ON
7	40	25	OFF
8	40	25	ON

Model parameter optimization was performed in order to minimize model artifacts as indicated by linear streaks in the lee of obstacles. Delft University of Technology researchers suggested that the directional spreading coefficient ('dd') should be maximized for accurate representation of wave energy in the lee of obstacles and diffraction effects should be explored.

3.3. SNL-SWAN Model Optimization Results

Model parameter optimization results are shown in Figure 9 and are summarized here. Note the presence of linear streaks that occurred when the 15° directional resolution parameter value was used. These streaks were caused by averaging model results into only 24 directional bins (every 15° over 360°). The linear streaks associated with the 15° directional resolution were reduced when 9° directional resolution (40 directional bins) was incorporated. No further increase in directional resolution was possible for the present model domain due to the relatively small computational grid size for the smallest modeled WEC devices. High resolution directional binning coupled with small computational grid size (8 m or less) was not possible due to limitations in model memory allocation for the high resolution grid.

Increased directional spread ('dd' equal to 25 as compared to 'dd' of 10) resulted in the influence of the WEC array being more focused directly in the lee of the obstacles. This is best illustrated in **Error! Reference source not found.** (Dirtn Spread = 25; Dirtn bin = 15deg; Diffr ON and Diffr OFF). Both of these figure panels show focused wave height reduction extending to the shoreline directly in the lee of the WEC array. In comparison, model runs that employed a dd value of 10 resulted in wave reduction effects that were more spread out laterally along the shoreline.

The effects of diffraction included larger wave heights at the edges of WEC influence (i.e. less difference in H_s between model runs without and with WECs and in some cases, increased wave height at the edges of WEC array influence), smaller wave heights directly in the lee of the WEC array, more pronounced wave height reduction effects from the WEC array toward the shoreline, and additional streak effects in the lee of the WEC array, seen as vertical lines in Figure 10.

Given the results of model parameter optimization runs, it was determined that diffraction was not accurately represented by the SWAN model for the purposes described here. In SWAN, the computation of diffraction is simplified to reduce computing requirements. Diffraction

computations involve a phase-decoupled approach to simulate the qualitative behavior of spatial redistribution and changes of wave direction (SWAN, 2011). As such, SWAN diffraction can result in the edge effects observed in model optimization simulations as shown in **Error! Reference source not found.** and **Error! Reference source not found.**. Generally, diffraction should be used in areas where variations in wave height are large within a horizontal scale of a few wave lengths. Additionally, higher directional resolution ('mdc' equal to 40) was recommended (Delft University of Technology, pers. comm., 2013). Therefore, subsequent SNL-SWAN model runs will be mindful of the results from this optimization study. Further sensitivity analysis of 'dd' is described for a variety of WEC device types in Section 4.

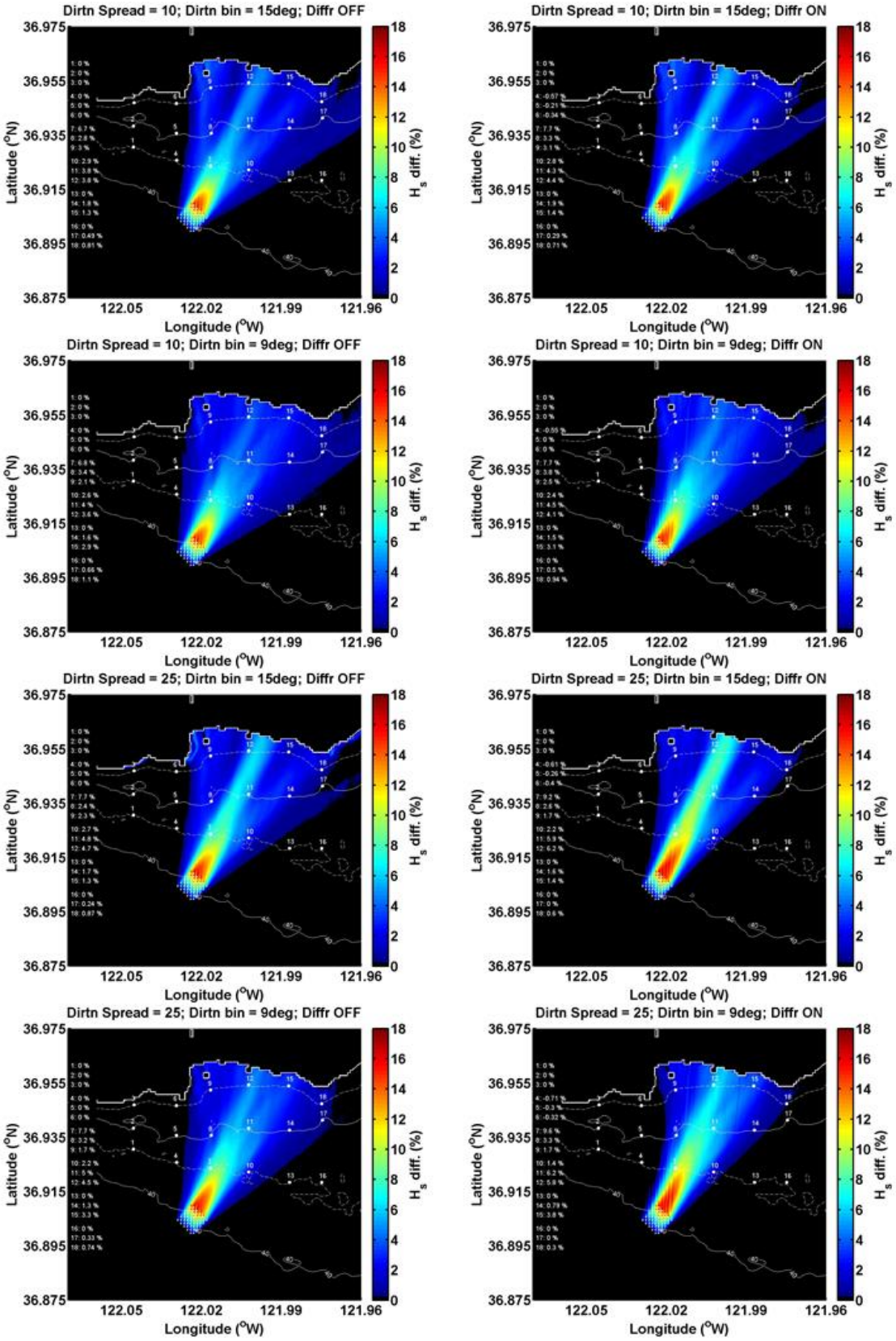

Figure 9. Percent difference in Hs between model optimization with and without WECs.

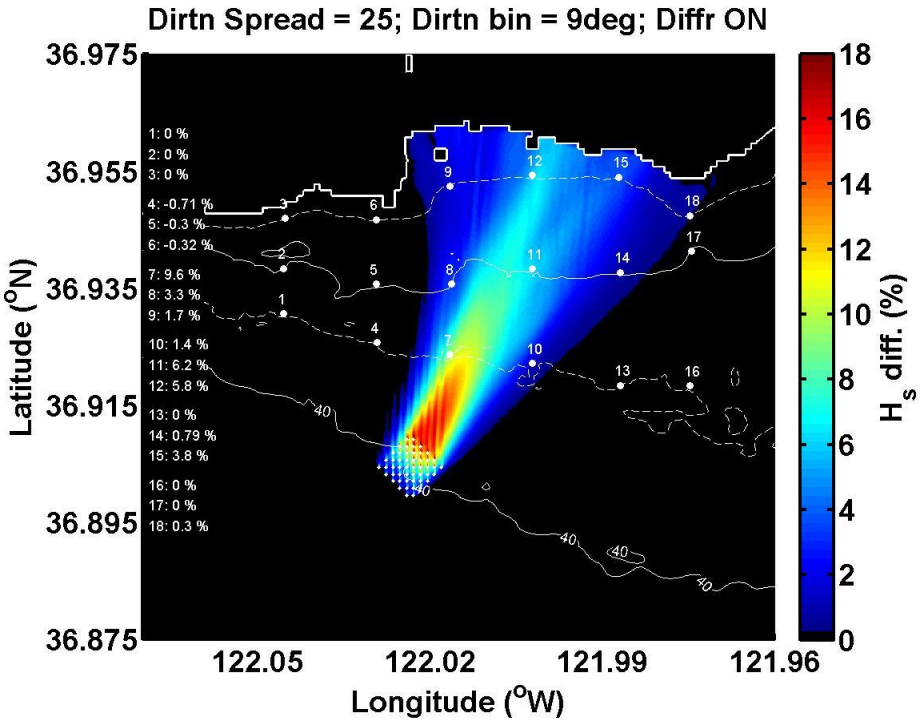

Figure 10. Percent difference in Hs between model optimization with and without WECs illustrating diffraction streak effects.

4. SNL-SWAN SENSITIVITY ANALYSIS – PART 1

4.1. Sensitivity Analysis Model Set-Up – Part 1

Three SNL-SWAN model grids were nested to predict the propagation of deep-water waves from offshore of Monterey Bay, CA, to near-shore Santa Cruz, CA. The Monterey Bay, Santa Cruz, and WEC SNL-SWAN model domains are shown in Figure 11. The Monterey Bay and Santa Cruz computational grids were the same as described in Section 2.1. The Monterey Bay model resolution was approximately 0.001° degrees in latitude and longitude and it was run as a stationary model. Directional wave energy spectra conditions were exported from the coarse resolution model and used as boundary conditions for the nested, fine resolution Santa Cruz model.

The grid resolution of the nested Santa Cruz model domain computational grid was approximately 0.00025° degrees in latitude and longitude. The wave spectrum boundary conditions were applied along the offshore boundaries of the Santa Cruz SNL-SWAN model domain. The nested grid model was also implemented as a stationary model. Directional wave energy spectra conditions were exported from the Santa Cruz model domain and used as boundary conditions for the nested, finest resolution model (herein referred to as the WEC model domain).

The grid resolution of the nested WEC model domain was approximately 0.00010° degrees in latitude and longitude (approximately 10 m in x and y). This grid size was smaller than the full-scale WEC devices modeled in this study. In SWAN and SNL-SWAN, obstacles must cross computational grid points in order for them to be accounted for in wave propagation simulation. By specifying a computational grid size that is smaller than the full-scale WEC devices for which the power matrices are provided, it was ensured that obstacles crossed at least one grid point. The Santa Cruz model wave spectrum boundary conditions were applied along the offshore boundaries of the WEC SNL-SWAN model domain. The inner nested grid model was also implemented as a stationary model.

See Section 2.1 for a description of the WEC array and model output locations.

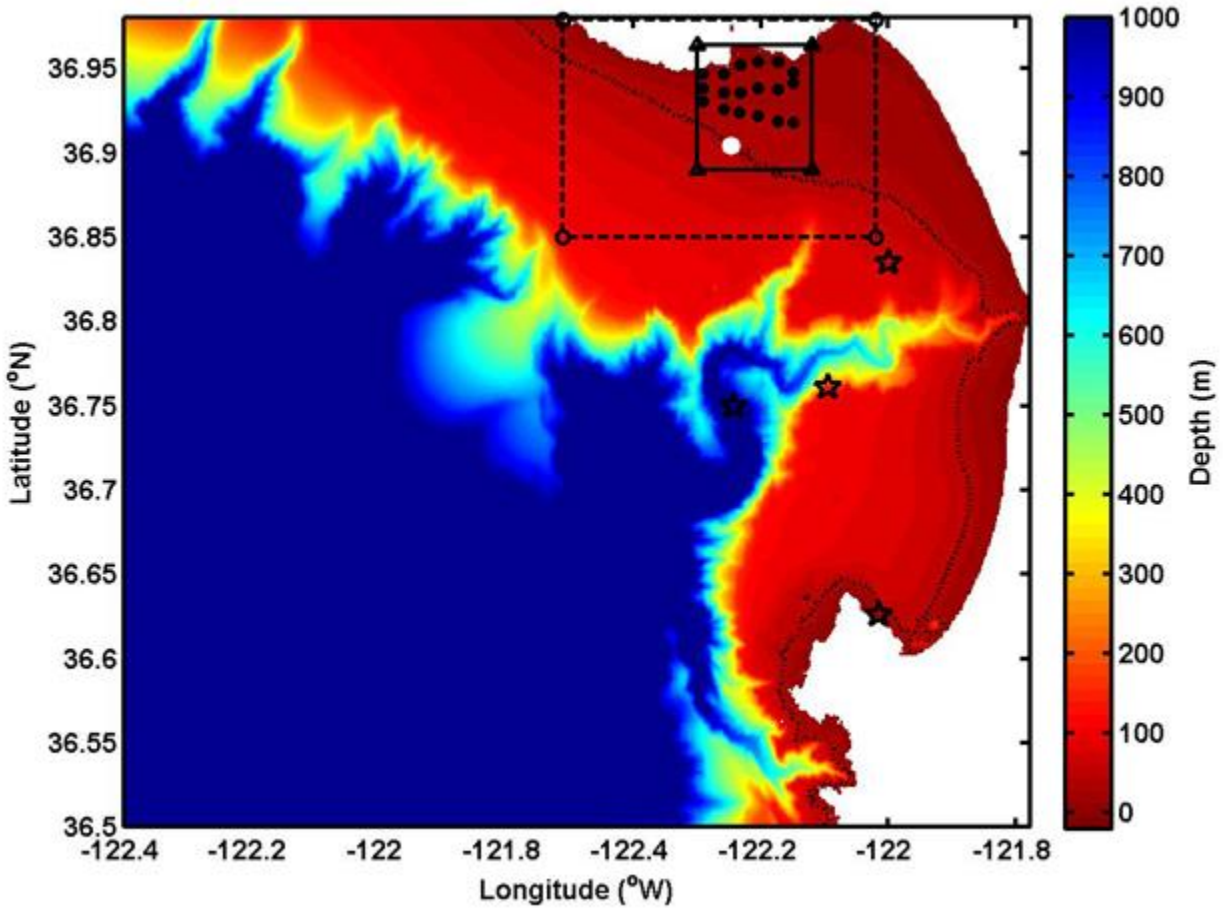

Figure 11. SNL-SWAN sensitivity analysis three-domain nested model domain. NDBC buoys are shown as stars. The white dot indicates the simulated WEC array and black dots are model evaluation locations.

4.2. Sensitivity Analysis Parameters – Part 1

The evaluation of the near- and far-field effects of WEC devices and arrays on the near-shore environment was accomplished by assessing wave property changes at the 18 model output locations (Figure 3), and the horizontal extent over which these changes are expected. The potential wave property changes in proximity to the nearest shoreline (e.g. Santa Cruz, CA) were explored in a sensitivity analysis by simulating three WEC device types, two incident wave heights, two incident wave periods, three frequency distribution spreading coefficients (gamma), and three directional distribution spreading coefficients (dd) (Table 7).

A total of 108 model runs (36 for each WEC device type) were conducted using SNL-SWAN with Switch 1 and an additional 108 model runs were evaluated for SNL-SWAN Switch 2. Results were compared to 36 model runs conducted with no obstacles. The initial mean wave direction of 205° was held constant for all model runs. Additionally, all model runs included an

array of 10 WEC devices (obstacles) with zero wave energy reflection allowed, and centered on the 40 m depth contour, as shown in Figure 2.

The sensitivity analysis parameter values are indicated in Table 7. The three different WEC devices evaluated were: (1) Bottom-fixed oscillating flap (B-OF), (2) Floating two-body heaving converter (F-2HB), and (3) Floating oscillating water column (F-OWC). The diameter of each WEC device was: (1) 26 m, (2), 20 m, and (3) 50 m (maximum of length and width) (Babarit et al., 2012). The power matrix for each device was computed by following Babarit et al. (2012).

Based on the data analyzed from NOAA NDBC buoy #46042, the mode of the wave heights and periods, 1.7 m and 12.5 sec, respectively, and the 95 percentile wave heights and periods, 3.5 m and 16 sec, respectively, were selected for the two incident wave height and wave period conditions. Gamma (frequency spreading coefficient) was varied between 1, 3.3, and 10 and dd (directional spreading coefficient) was specified as 2, 10, or 25.

Table 7. Sensitivity analysis parameter values.

Parameter	Values
WEC Device Type	['B-OF', 'F-2HB', 'F-OWC']
Initial Wave Height (m)	[1.7, 3.5]
Initial Wave Period (sec)	[12.5, 16]
Frequency Distribution Spread	[1, 3.3, 10]
Directional Distribution Spread	[2, 10, 25]

4.3. Sensitivity Analysis Results – Part 1

Model results were retained for each model run listed in Appendix A (216 runs in total – 108 for Switch 1 and 108 for Switch 2). Results included propagated wave heights, wave periods, wave directions, and near-bottom orbital velocities at all grid points in the model domains. Further, the same wave properties were extracted at each of the 18 distinct model output locations to facilitate simple point-to-point comparison.

Figure 12 through Figure 22 illustrate the results from sensitivity analyses. The results are surface-to-surface comparisons, comparing the modeled scenario results to the baseline scenario results, where the baseline scenario does not include obstacles. In Figure 12 through Figure 17, black coloring indicates no (or negligible) change in wave parameter from the baseline scenario. Color bars are included in each figure to define the amount of change, where change is defined as a percentage change from the baseline scenario (Eq. 1). Recall that a positive change indicates a decrease in the value of the wave parameter in the presence of a WEC array and *vice versa*. In addition, the percentage change computed at each of the 18 model output locations is listed as text in each sub-figure, adjacent to the output location number; this allows for rapid comparisons from case to case.

4.3.1. Significant Wave Height

Results of significant wave height predictions from the sensitivity analysis using Switch 1 and 2 are shown in Figure 12 and Figure 13, respectively. Figure 14 shows additional results for Switch 2 (T_p = 16 s). The model parameters (WEC device type and boundary conditions) are indicated above each subplot. Immediately evident from examination of these figures is that there appeared to be an issue with running SNL-SWAN Switch 2 with an initial wave period of 16 s and the B-OF and F-2HB device types (Figure 14). Wave height actually *increased* in the lee of the WEC array during these conditions. Additionally, the resultant transmission coefficients for the B-OF buoy and for the F-2HB buoy with wave period of 16 s were completely unreasonable (values above 1.0 or negative values). The root of this problem was an error in the SNL-SWAN code in passing variables from the model to the output PRINT file. This error has since been debugged and fixed in the current version of SNL-SWAN (Appendix A; Figure A 1).

Switch 1 and Switch 2 results for model runs with initial wave period of 12.5 sec were comparable. Wave height decreases of between zero and 3% were observed at the 18 output locations when compared to the baseline scenario. The largest wave height decreases directly in lee of the WEC arrays and the longest horizontal impact (i.e. largest effect toward the shoreline) occurred for the B-OF WEC device type. The widest horizontal (along-shore) effects were largest for the F-OWC device type, which makes intuitive sense given that these are the largest devices.

4.3.2. Near-Bottom Orbital Velocities

Near-bottom orbital velocities (e.g. wave-driven currents) were directly proportional to the surface wave expression (i.e. significant wave height). Decreased wave heights caused a decrease in near-bottom orbital velocities, potentially altering the ambient wave-driven currents in a near-shore environment. Consequently, the percentage differences of the near-bottom orbital velocities were essentially equivalent to those computed from the significant wave height model scenarios. Figures of near-bottom orbital velocity percentage differences are not included since they were equivalent to Figure 12, Figure 13, and Figure 14.

4.3.3. Peak Wave Periods

The percentage changes in peak wave periods during this study were negligible, as shown in Figure 15 (Switch 2 results are identical and therefore are not shown). The reason for this was twofold. First, within the model parameters, the frequency bin resolution may have been too large to register small changes in wave periods (small changes in frequency would not cause a change in frequency bin in model space). Second, since the model obstacles were "absorbing" the same percentage of wave energy from all wave frequencies (i.e. because the transmission coefficient is frequency-independent), there would be no change in peak wave energy; the dominant wave energy would not shift to an alternate frequency(ies). Therefore, in the present study, no change (or negligible change) would be observed. [Note that up to -30% differences were found in peak wave periods for Switch 2 runs with 16 sec initial wave period and the B-OF and F-2HB WEC devices; this issue is described above and has since been resolved.]

4.3.4. Mean Wave Directions

Changes in mean wave directions are illustrated in **Error! Reference source not found.**Figure 16 and Figure 17 as degrees changed (as opposed to percentage changes) for easy interpretation. Negative changes (blue) indicate clockwise (CW) rotation of wave direction. Positive changes (red) indicate counter-clockwise (CCW) rotation. Rotation, when it occurred, was relatively large, for the same reasons described for peak periods: the directional bin spacing was 15-degrees. Any changes less than this were indeterminable by the model.

Recall from Chang et al. (2014) that mean wave directions were most affected by the largest WEC device array(s) (e.g., greater than 100 WEC devices), which caused the largest horizontal extent wave shadowing effects in lee of the array(s). As a result of transmission coefficient and depth contour variation, mean wave directions were altered, but changes were minor. For the present study, only 10 WEC devices were modeled in an array; hence directional changes were for the most part negligible throughout the WEC model domain. Up to ~-15° differences were found near the 10 m depth contour for Switches 1 and 2 and also directly in the lee of the B-OF WEC array when using Switch 1.

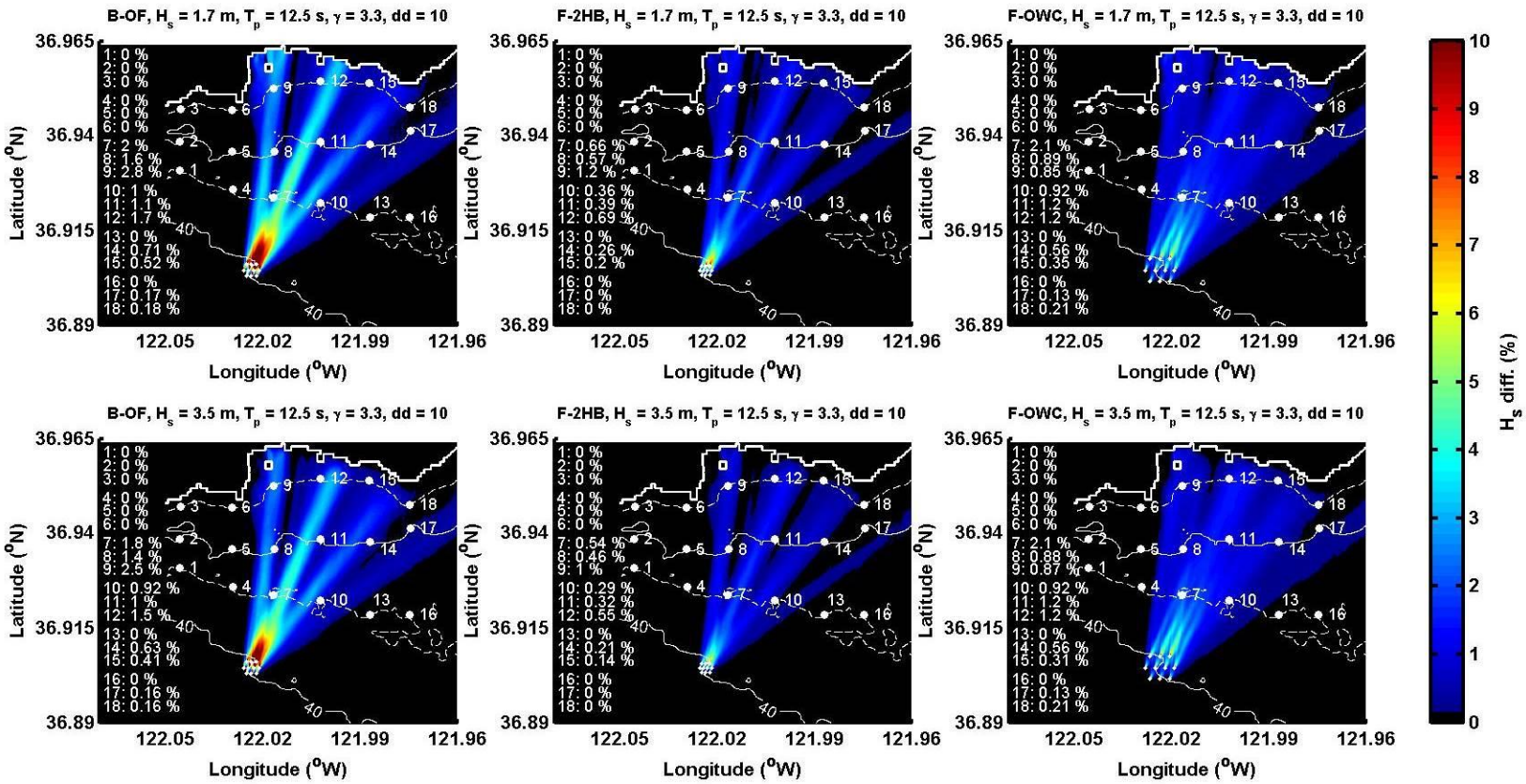

Figure 12. Significant wave height percentage decrease as a result of varying model parameters (as indicated above each panel) using SNL-SWAN Switch 1. The WEC array was centered on the 40 m depth contour and comprised of 10 devices. Note that the device diameters represented in the figure are not to scale.

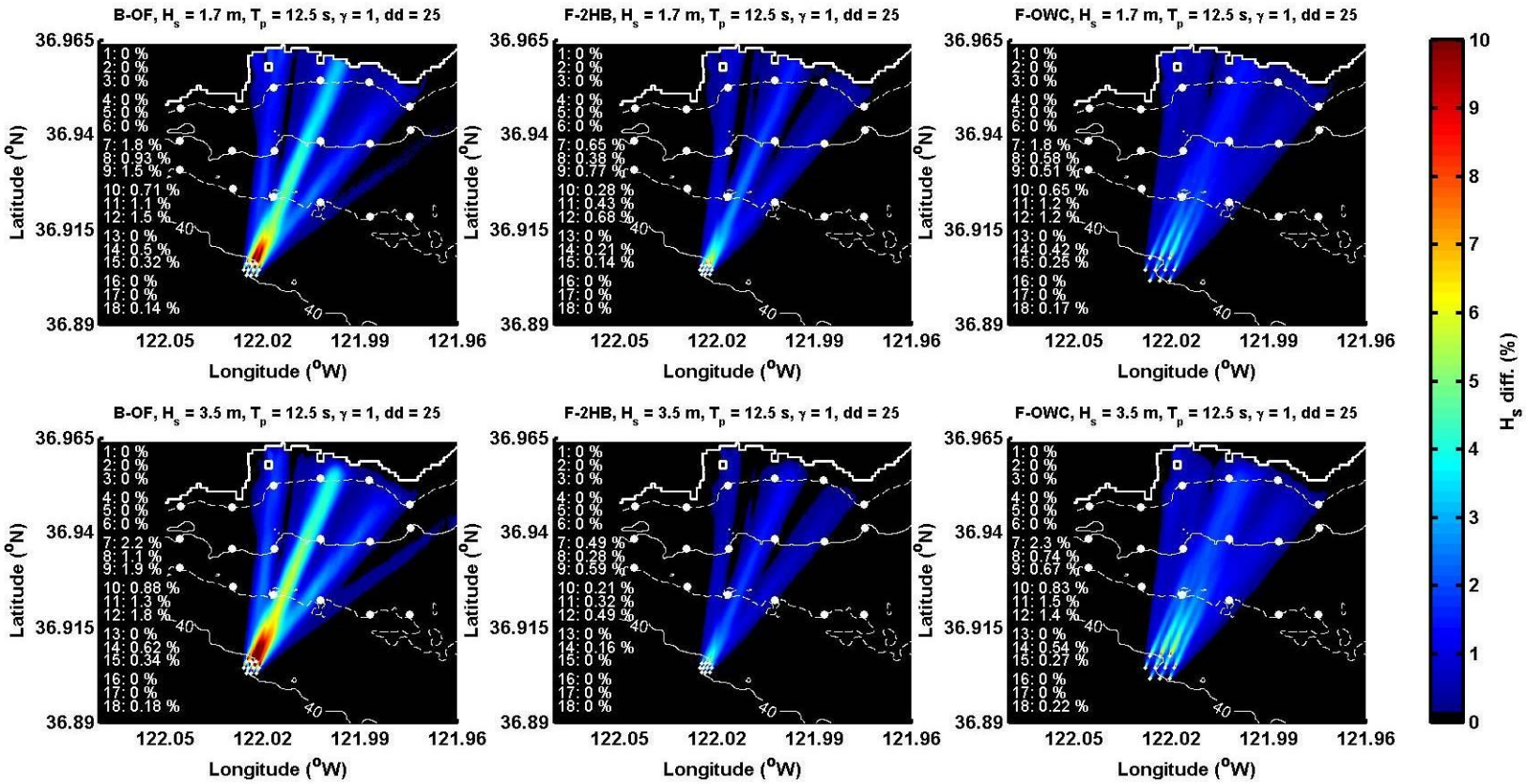

Figure 13. Same caption as for Figure 12 but using Switch 2.

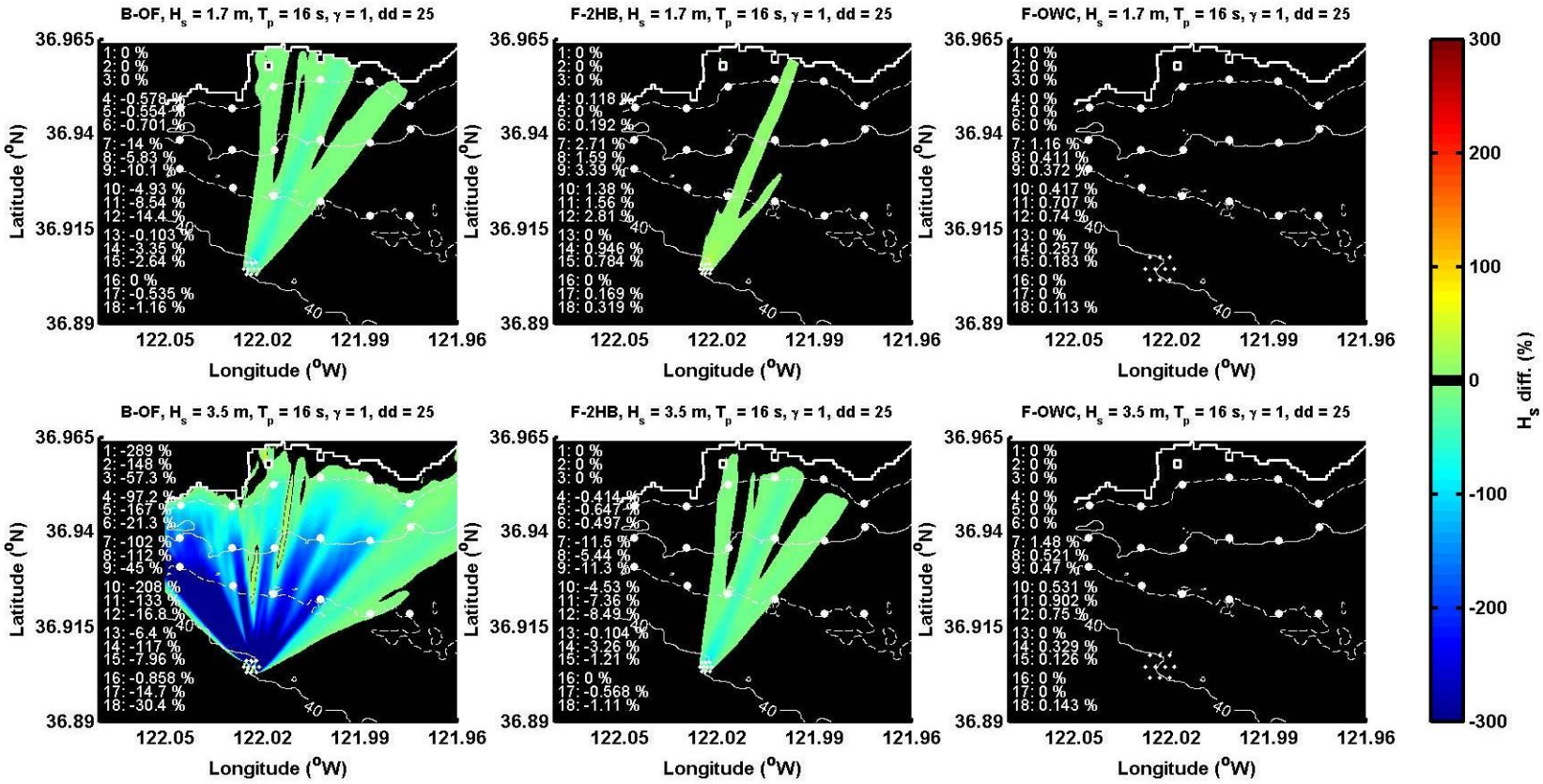

Figure 14. Same caption as for Figure 12 but for Switch 2 and T_p = 16 s, shown to illustrate the issue with particular Switch 2 model runs.

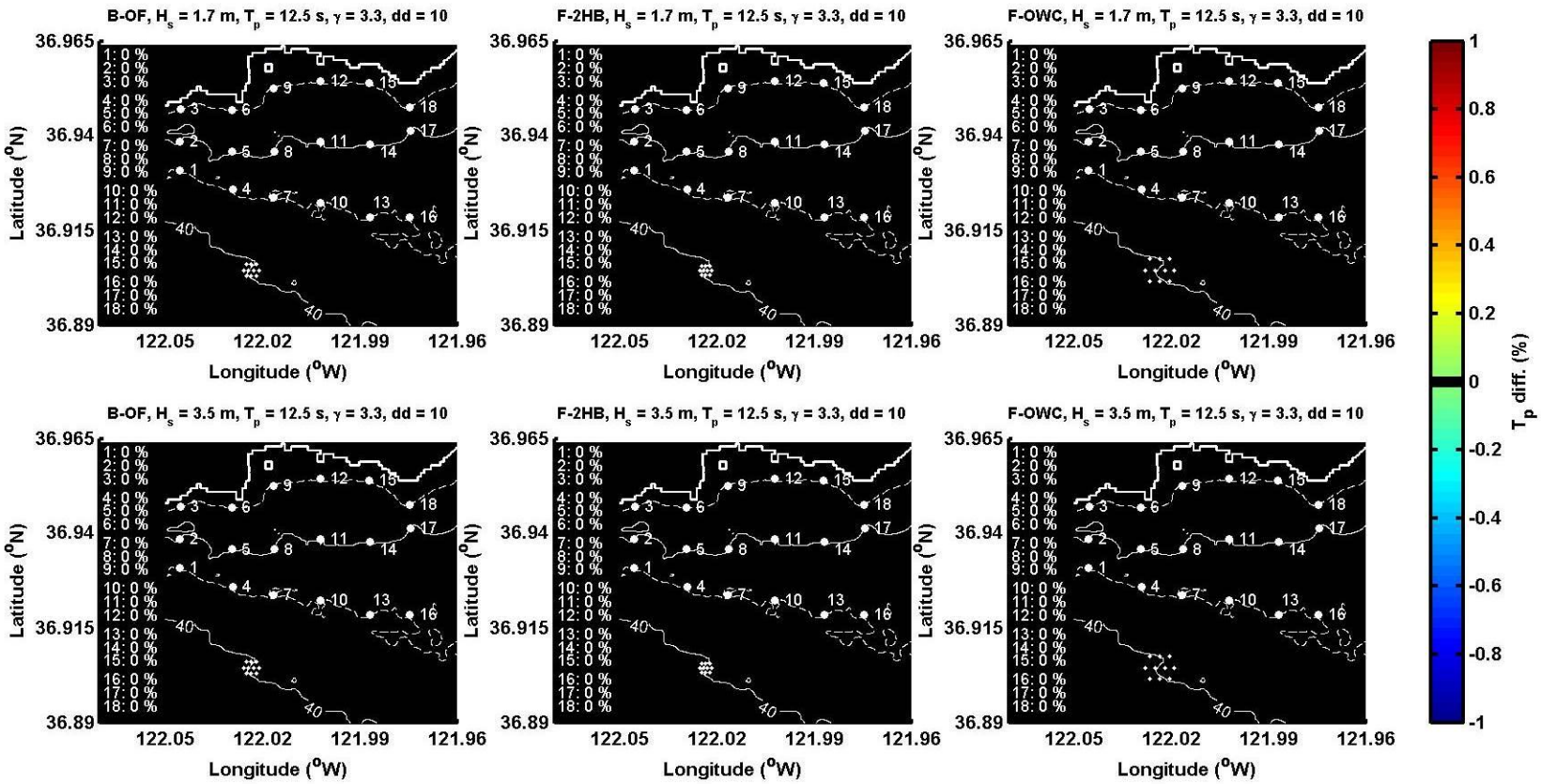

Figure 15. Peak wave period percentage decrease as a result of varying model parameters, as indicated.

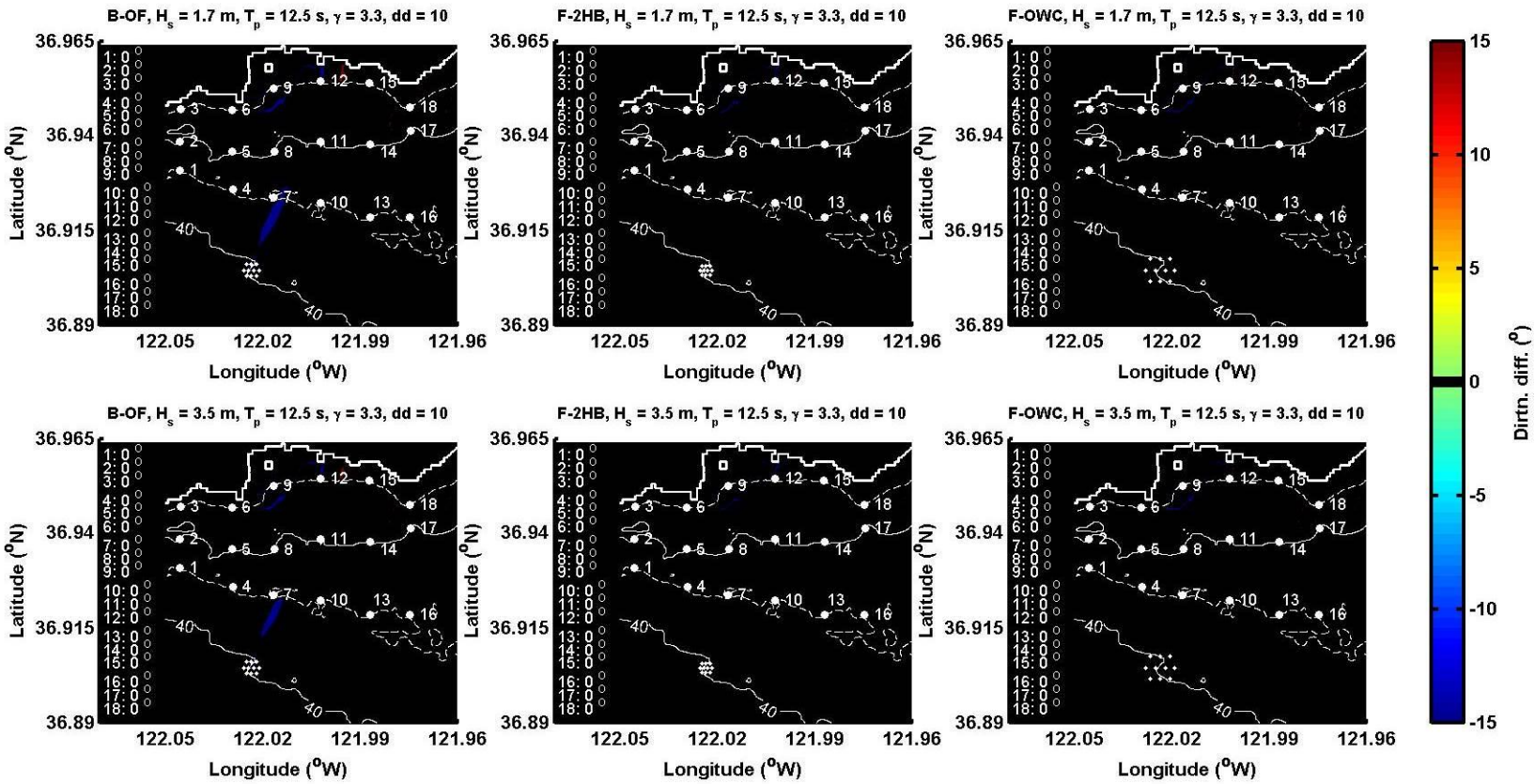

Figure 16. Mean wave direction decrease (degrees) as a result of varying model parameters, as indicated, for SNL-SWAN Switch 1.

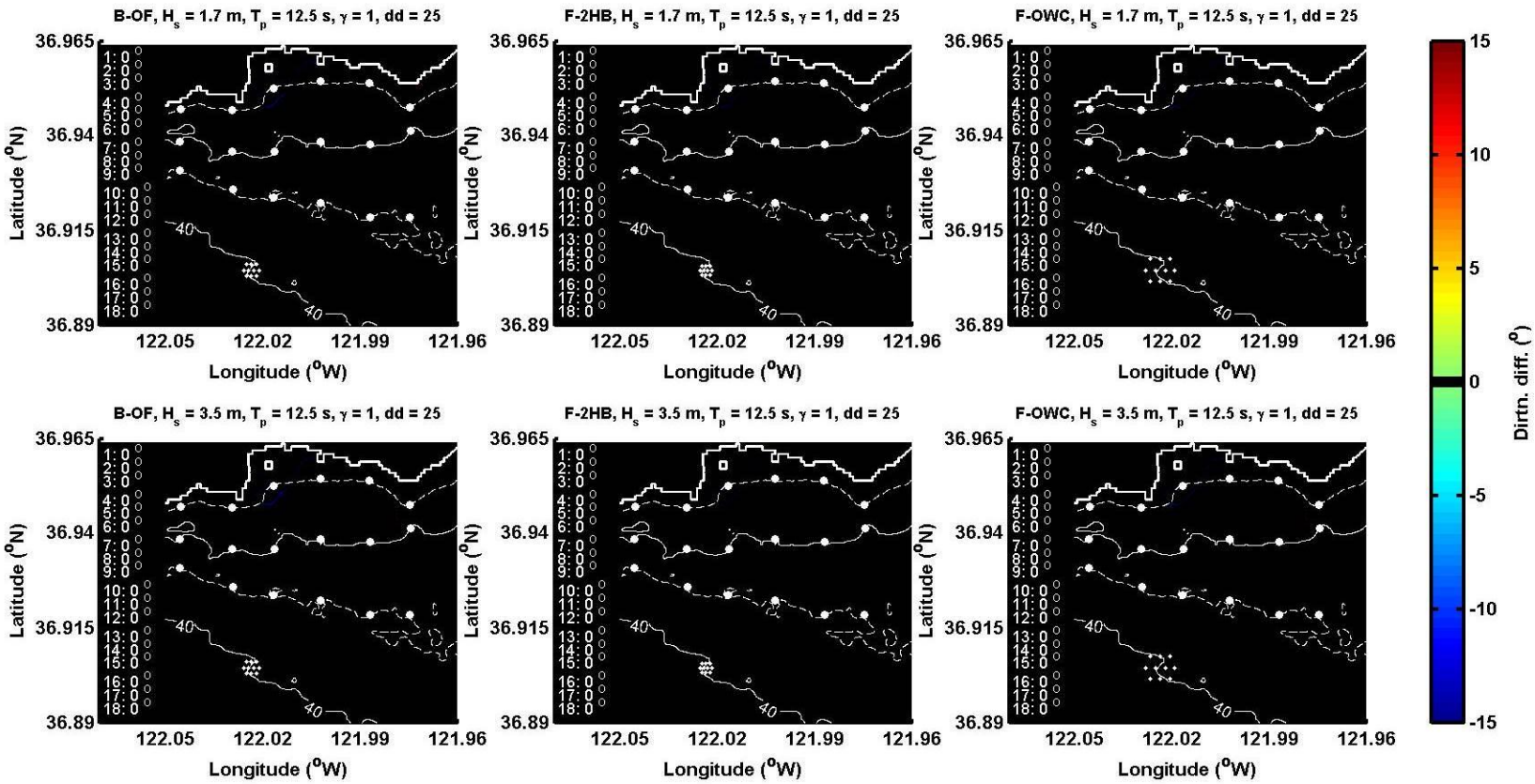

Figure 17. Same caption as Figure 16 but for SNL-SWAN Switch 2.

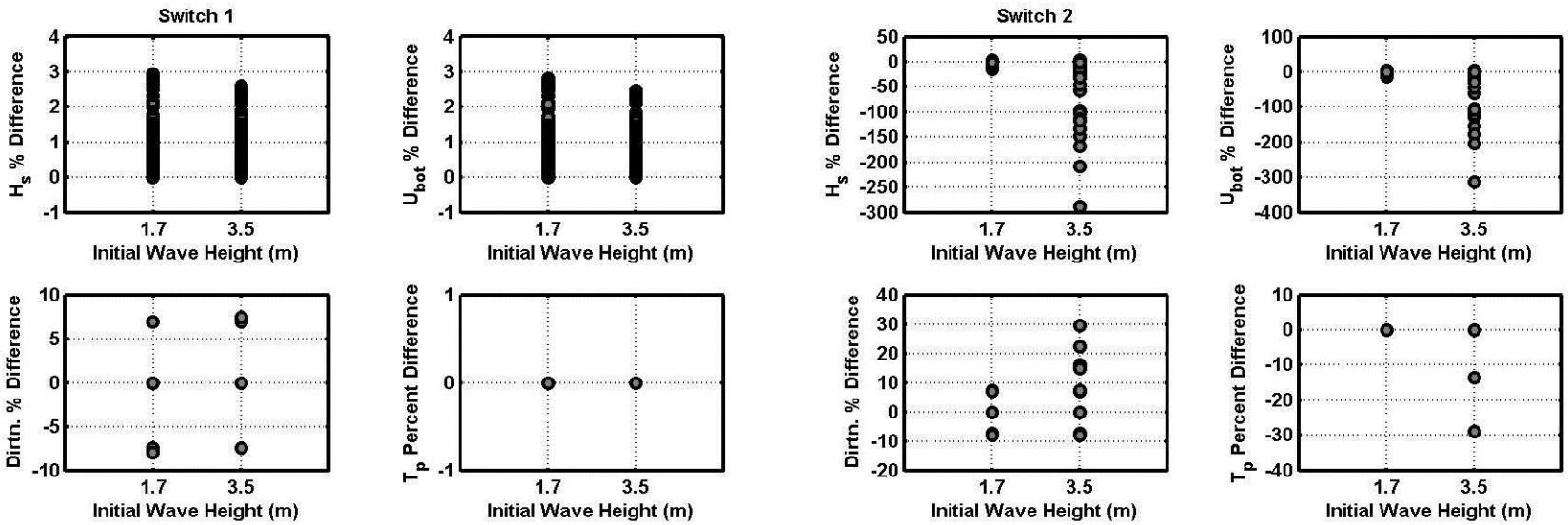

Figure 18. Variation in wave properties versus wave height boundary conditions. The left four panels are the results from using Switch 1 and the right four panels are from Switch 2. Note the differences in the y-axes.

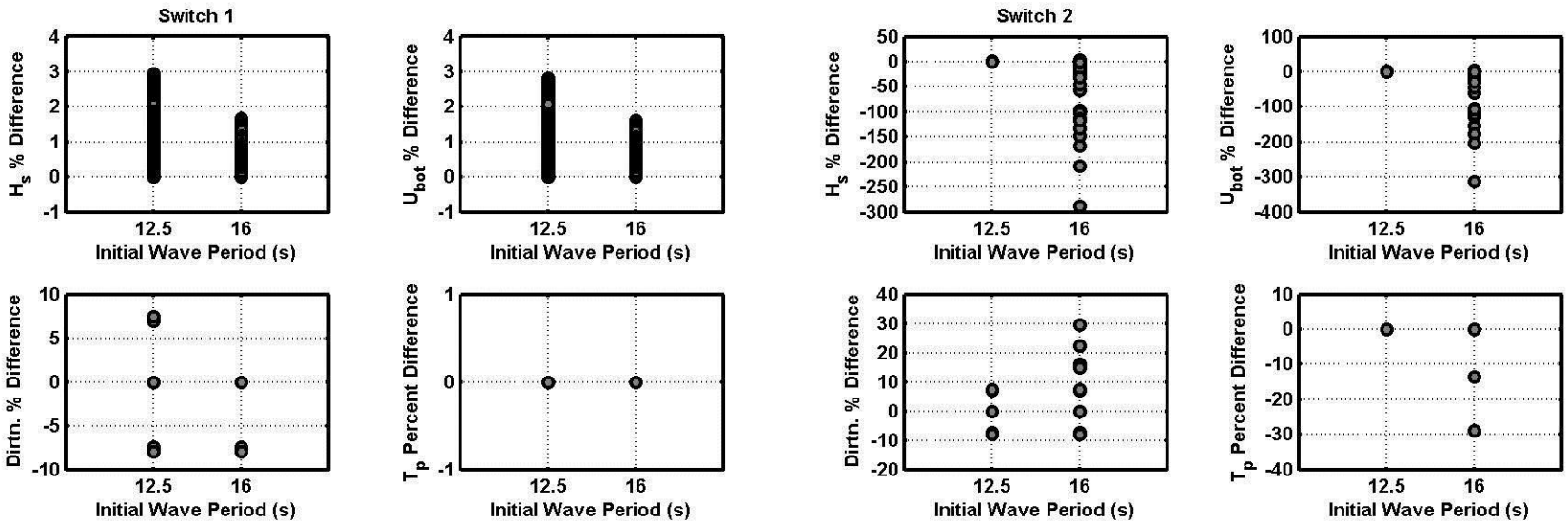

Figure 19. Variation in wave properties versus wave period boundary conditions for all 216 model runs. The left four panels are the results from using Switch 1 and the right four panels are from Switch 2. Note the differences in the y-axes.

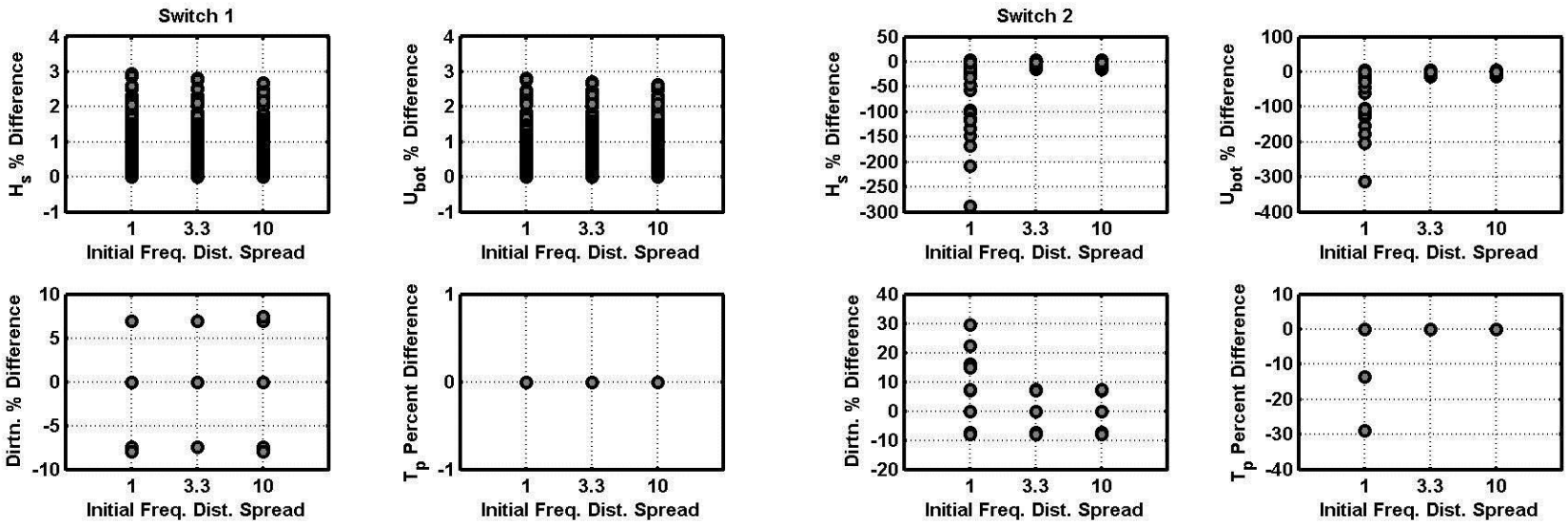

Figure 20. Variation in wave properties versus frequency distribution spread for all 216 model runs. The left four panels are the results from using Switch 1 and the right four panels are from Switch 2. Note the differences in the y-axes.

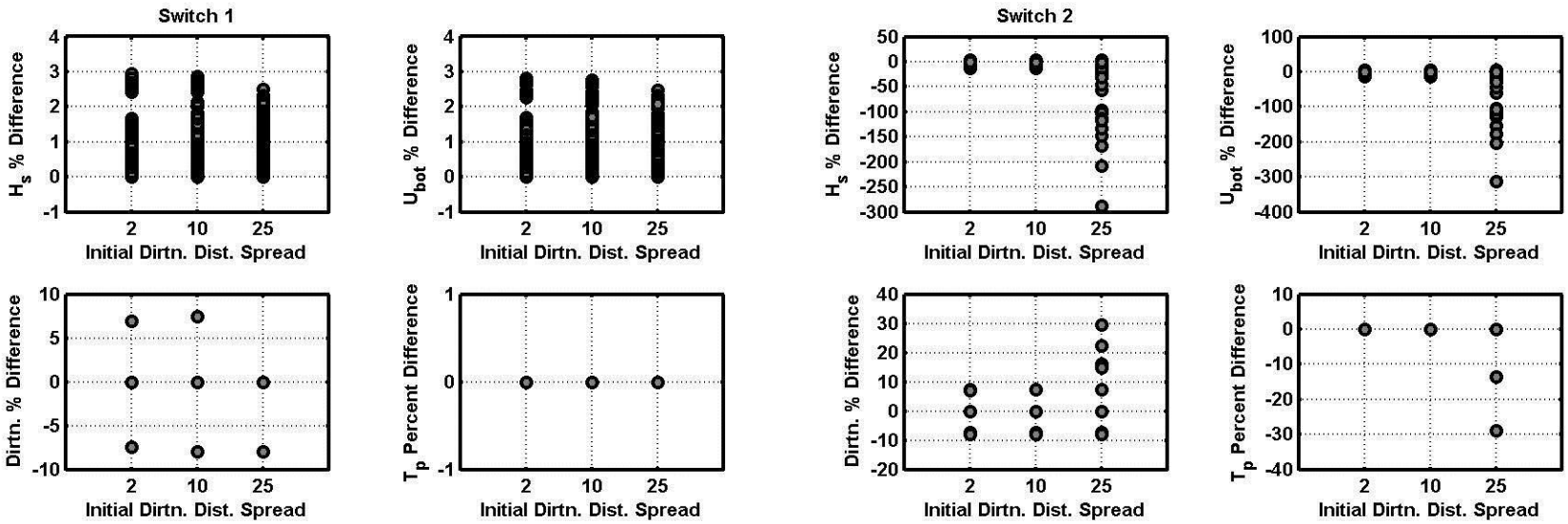

Figure 21. Variation in wave properties versus directional distribution spread for all 216 model runs. The left four panels are the results from using Switch 1 and the right four panels are from Switch 2. Note the differences in the y-axes.

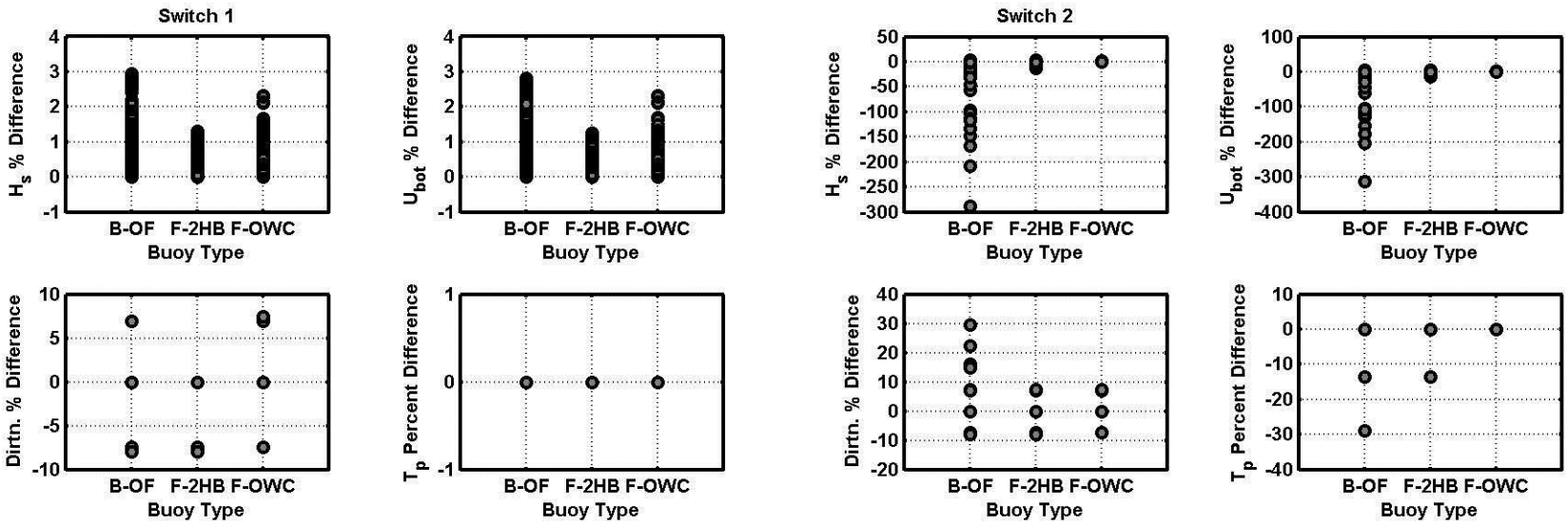

Figure 22. Variation in wave properties versus WEC device type for all 216 model runs. The left four panels are the results from using Switch 1 and the right four panels are from Switch 2. Note the differences in the y-axes.

4.3.5. Results Summary

The total variation in all wave conditions versus initial boundary condition wave height for all scenarios modeled in the present study is illustrated in Figure 18. The shape of the scatter plots and degree of vertical spreading that exists for each constant parameter were indications of the model sensitivity to that parameter. This figure illustrates that both wave height and near-bottom velocity were subject to small variations, decreasing as initial wave heights increased from 1.7 to 3.5 m. Wave direction was affected consistently for all wave heights; and wave period was not affected (or negligibly affected) by varying wave height.

Similar results were observed in Figure 19 through Figure 22, which indicate the range of changes anticipated as a function of initial wave period, frequency distribution spread, directional distribution spread, and WEC device type. Wave height variability generally decreased with increasing initial wave period, increasing frequency distribution spread, and increasing directional distribution spread.

Another means of viewing the model results is presented in Figure 23 through **Error! Reference source not found.** (Switch 1 only; Switch 2 results are similar and therefore not shown), which allow determination of the model parameters which have the greatest effect on the specific wave properties. From Figure 23, it is evident that the largest wave height (and bottom-orbital velocity; not shown) variation is expected when the initial boundary condition wave height and period was 1.7 m and 12.5 s, frequency distribution and directional distribution spreads were 1 and 2, and the WEC device type was B-OF. Mean wave directions varied the least for 16 s initial wave period, directional distribution spread of 25, and the F-2HB WEC device type (Figure 24). The peak wave periods were not affected (or were negligibly affected) by variation of the parameters (Figure 25).

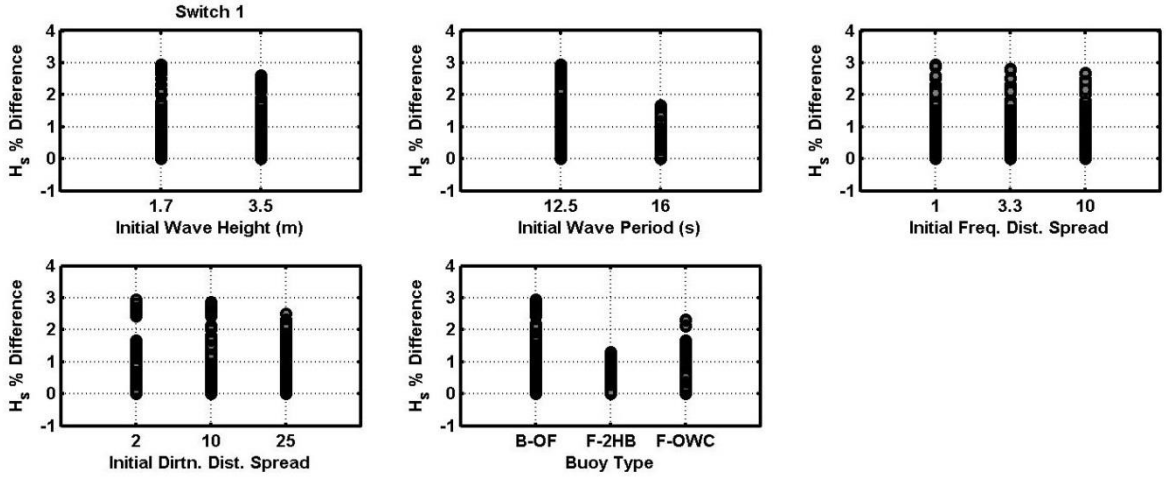

Figure 23. Variation in significant wave height for all varied model parameters.

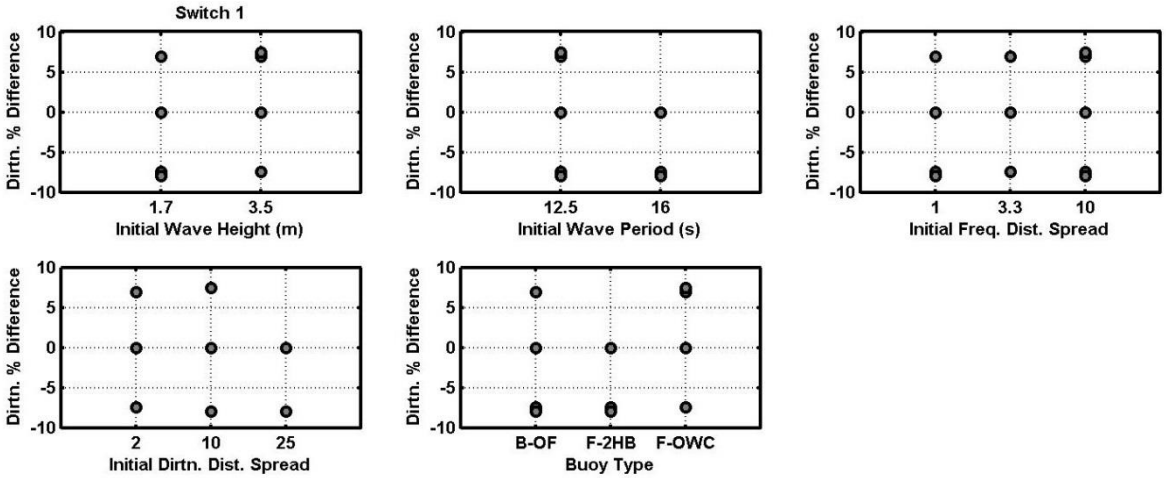

Figure 24. Variation in mean wave direction for all varied model parameters.

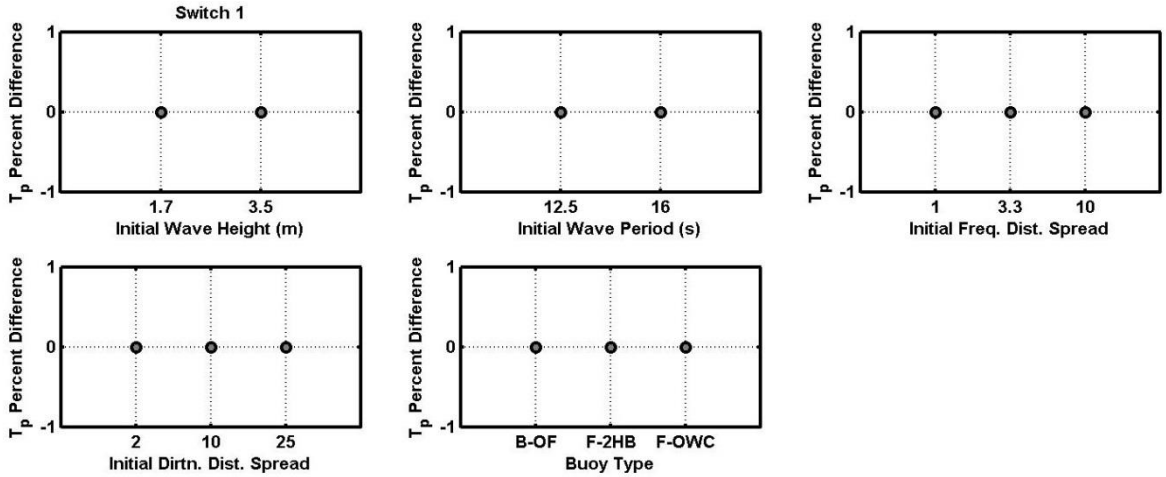

Figure 25. Variation in peak wave period for all varied parameters.

These results ultimately illustrated, that, given the present model setup, the wave heights (and associated near-bottom orbital velocities) and direction, as well as WEC device type showed consistent differences of up to ±10% between baseline and modeled conditions for selected sensitivity analysis variables. Wave periods did not appear to be sensitive to changes in parameters. However, additional analysis is required to fully explore the model sensitivity of peak wave period and mean wave direction to the varying of the parameters.

Model output locations located to the East and West showed relatively little to no change in wave heights compared to the baseline scenario. The largest wave height differences were observed downstream of the array near the array centerline (output locations 7-12), where the largest wave shadowing effects were predicted. Depending upon the parameters selected during

each scenario, additional model output locations may also indicate large changes in wave heights.

5. SNL-SWAN SENSITIVITY ANALYSIS – PART 2

5.1. Sensitivity Analysis Parameters – Part 2

Model sensitivity analysis was performed using SNL-SWAN in order to understand model behavior in the vicinity of a variety of different WEC devices, sizes, WEC spacing within an array, and number of WECs in an array. The potential wave property changes in proximity to the Santa Cruz, CA shoreline were explored by simulating eight different WEC device types with seven different diameters (**Error! Reference source not found.**) arranged in honeycomb/diamond-shaped arrays of 10, 50, or 100 WEC devices that were spaced 4, 6, or 8 diameters apart. The power matrix for each of the eight devices was computed by following Babarit et al. (2012).

Table 8. WEC device types and associated diameters (maximum of length and width; from Babarit et al., 2012) simulated for SNL-SWAN model sensitivity analysis.

WEC type	Abbreviation	Diameter (m)
Small bottom-referenced heaving buoy	Bref-HB	5*
Bottom-fixed heave-buoy array[#]	B-HBA	5
Bottom-referenced submerged heave-buoy[#]	Bref-SHB	7
Floating heave-buoy array[%]	F-HBA	8
Floating three-body oscillating flap device	F3 OF	9.5
Floating two-body heaving converter	F-2HB	20
Bottom-fixed oscillating flap	B-OF	26
Floating oscillating water column	F-OWC	50

* The Bref-HB size was listed as 3 m; however it was specified as 5 m in SNL-SWAN model runs due to limitations on computational grid size.

[#]B-HBA and Bref-SHB were modeled as obstacles that extended throughout the water column although both are devices without surface expressions.

[%]F-HBA is a multi-body WEC, composed of any number of heaving buoys connected to a submerged structure. The actual dimension of F-HBA is dependent on the number of heaving buoys within its body. It was therefore modeled as a singular 8-m diameter obstacle.

5.2. Sensitivity Analysis Model Set-Up – Part 2

5.2.1 WECs larger than 15 m

The nested model domains for WEC devices greater than 15 m in diameter were the same as described in Section 3.1 and shown in Figure 1. However, the inner Santa Cruz model domain grid size was set equal to the size of the particular WEC device being modeled. This was to establish each device as equivalent to a model grid cell, which would simplify model performance evaluation and assessment.

5.2.2 WECs smaller than 15 m

WEC devices less than 15 m in diameter were modeled with a triple-nested SNL-SWAN model. The reason for this additional nested grid was due to model allocation limitations when attempting to model grid cells less than 15 m in dimension. The Monterey Bay, WEC, and Santa Cruz SNL-SWAN model domains are shown in Figure 26 and Figure 27. The coarse-grid Monterey Bay model domain resolution was approximately 100 m grid spacing in x and y. The model was run as a stationary model. Directional wave energy spectra conditions were exported from the coarse resolution model and used as boundary conditions for the nested, finer resolution model (herein referred to as the WEC model domain).

The grid resolution of the nested WEC model domain was equal to the modeled WEC device diameter. WEC devices that were 5 m in diameter required a smaller WEC domain due to model computational limitations. WEC devices between 6 m and 10 m required a larger WEC domain such that the entire WEC array of up to 100 devices would be accommodated. The WEC nested grid model was also implemented as a stationary model. The WEC model wave spectrum boundary conditions were applied along the southern offshore boundary of the Santa Cruz model domain. The boundary between the WEC domain and the Santa Cruz domain was extended sufficiently to the west in order to avoid boundary effects that may have negative effects on the 18 model output locations.

The grid resolution of the innermost Santa Cruz model domain computational grid was approximately 0.00025° degrees in latitude and longitude (approximately 25 m in x and y). The innermost Santa Cruz domain was also implemented as a stationary model.

A total of 144 model runs were conducted (72 for each of SNL-SWAN Switch 1 and 2). Results were compared to seven model runs conducted with no obstacles. The seven runs with no WECs represented each of the seven different device sizes. The initial wave conditions were: H_s = 1.7 m, T_p = 12.5 s, mean wave direction = 205°, frequency spread = 3.3, and directional spread = 25. These initial wave conditions were held constant for all model runs. Additionally, all model runs were conducted with 9° directional resolution (mdc = 40), zero wave energy reflection allowed, no diffraction, and the WEC array centered on the 40 m depth contour, as shown in Figure 2. Model sensitivity analysis parameters for each model run are summarized in Appendix B.

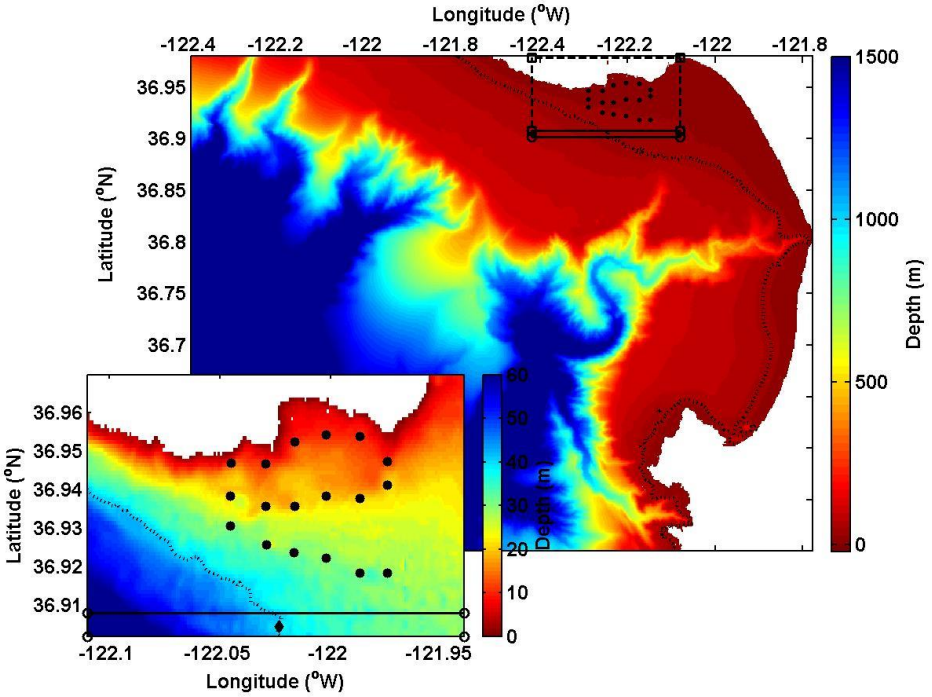

Figure 26. Monterey Bay, WEC (bounded by solid lines), and Santa Cruz (bounded on three sides – north, west, and east – by dashed lines) SNL-SWAN model domains for devices less than 6 m in diameter (40 m depth contour indicated by a dotted line). The inset shows a close-up view of the WEC and Santa Cruz domain (boundary between the two marked by the solid line).

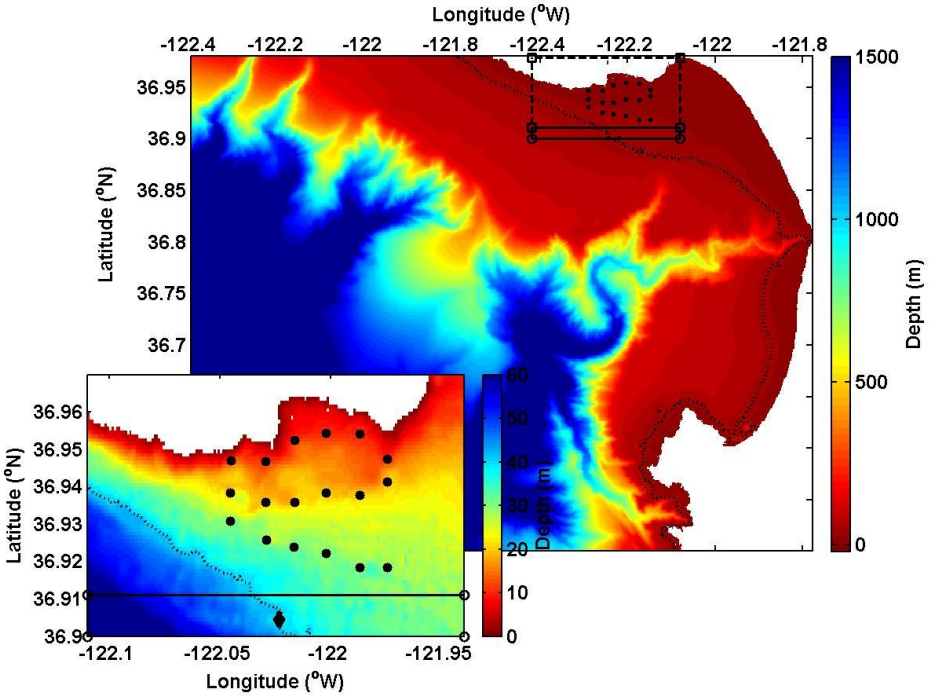

Figure 27. Same caption as Figure 26 but for devices between 6 m and 15 m in diameter.

5.3. Sensitivity Analysis Results – Part 2

Model results were retained for each model run. Results included propagated wave heights, wave periods, wave directions, and near-bottom orbital velocities at all grid points in the model domains. Further, the same wave properties were extracted at each of the 18 distinct model output locations to facilitate point-to-point comparison.

Figure 28 through Figure 30 illustrate the results from sensitivity analyses. The results are surface-to-surface comparisons, comparing the modeled scenario results to the baseline scenario results, where the baseline scenario does not include WEC devices. Black coloring indicates no change in wave parameter from the baseline scenario. Color bars are included in each figure to define the amount of change, where change is defined as a percentage change from the baseline scenario (Eq. 1).

5.3.1 Significant Wave Height

Results of significant wave height predictions from the sensitivity analysis for 50 F-2HB type WECs using Switch 1 and Switch 2 are shown in Figure 28 for comparison of the two switches (transmission coefficients resulting from the two switches are discussed further below). Switch 1 and Switch 2 results for model runs were comparable but not identical; likely due to effects of the interpolation of wave height and period when computing the RCW for Switch 2. Wave heights were slightly more reduced in the lee of 50 F-2HB WEC device types spaced six

diameters apart for Switch 1 as compared to Switch 2. Switch 2 simulations resulted in 0.1% more wave reduction for output locations 7, 8, 11, 12, and 18. Wave height decreases of between zero and 8% were observed for output locations to the northeast of the WEC array for Switch 1 and Switch 2 (Figure 28). The comparisons between Switch 1 and Switch 2 for the seven other WEC devices were similar.

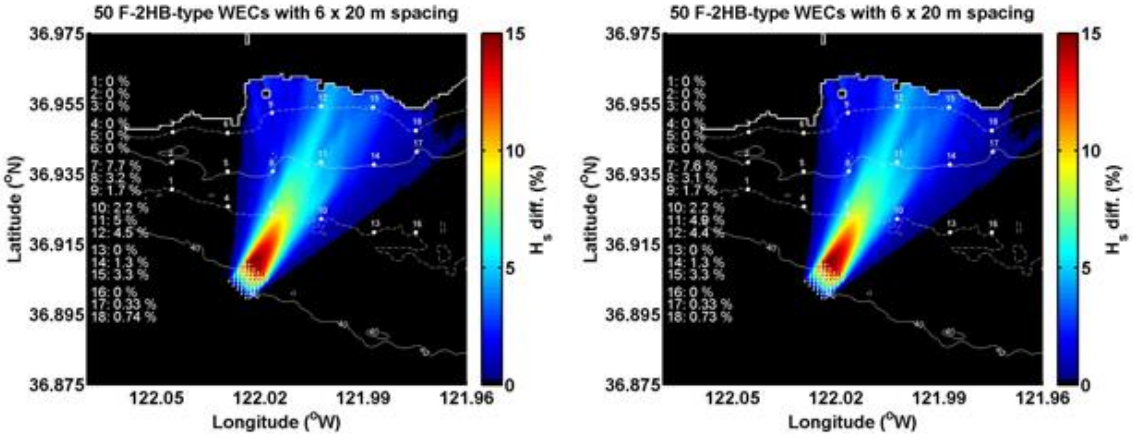

Figure 28. Significant wave height percentage decrease as a result of varying model parameters (as indicated above each panel) using SNL-SWAN Switch 1 (left) and Switch 2 (right). Note that the device diameters represented in the figure are not to scale.

Switch 1 model results for all eight WEC buoy types are shown in Figure 29 and Figure 30. Switch 2 results were similar and are not shown. The model parameters (number of WECs, WEC device type, WEC spacing, and WEC diameter) are indicated above each subplot.

For all eight device types, the largest wave height decreases were directly in the lee of the WEC arrays. In general, smaller devices had less impact on wave height as compared to larger buoy sizes. Exceptions to this statement were the Bref-SHB buoy (7 m), which exhibited wave height reductions of roughly equal magnitude as the B-HBA WEC type (5 m) and the F-OWC buoy (50 m), which had less of an impact on wave height than the 26 m B-OF device type (Figure 29 and Figure 30). The magnitude of wave height reduction was directly correlated to the WEC's power matrix values, with larger values resulting in more reduction in wave height and *vice versa*.

The largest spatial (horizontal or along-shore) wave reduction effects were observed with the F-OWC device, which makes intuitive sense given that these were the largest of the modeled devices and were thus also spaced furthest apart (i.e. blocking a larger percentage of the propagating waves). Recall that submerged buoys (B-HBA and Bref-SHB) were modeled as obstacles that extended throughout the water column; results could have been significantly different for these devices if simulated as obstacles covering only a portion of the lower water column.

Figure 31 summarizes model sensitivity to the following varied parameters: WEC buoy type, number of WEC devices in the array, and WEC spacing. Variability in wave height percent differences was largest for buoy type, i.e. the model was most sensitive to WEC device type (and WEC size with the exception of the F-OWC buoy). The power matrix associated with each WEC was generally scaled to WEC size (i.e. larger buoys exhibited greater power generation as compared to smaller devices), with the exception of the F-OWC buoy. WECs with higher power generation resulted in greater wave height reduction. Wave height reduction was strongly sensitive to the number of WEC devices but relatively insensitive to WEC spacing. As expected, the larger the number of WECs in the array, the greater the difference between modeled wave height with and without obstacles (Figure 31).

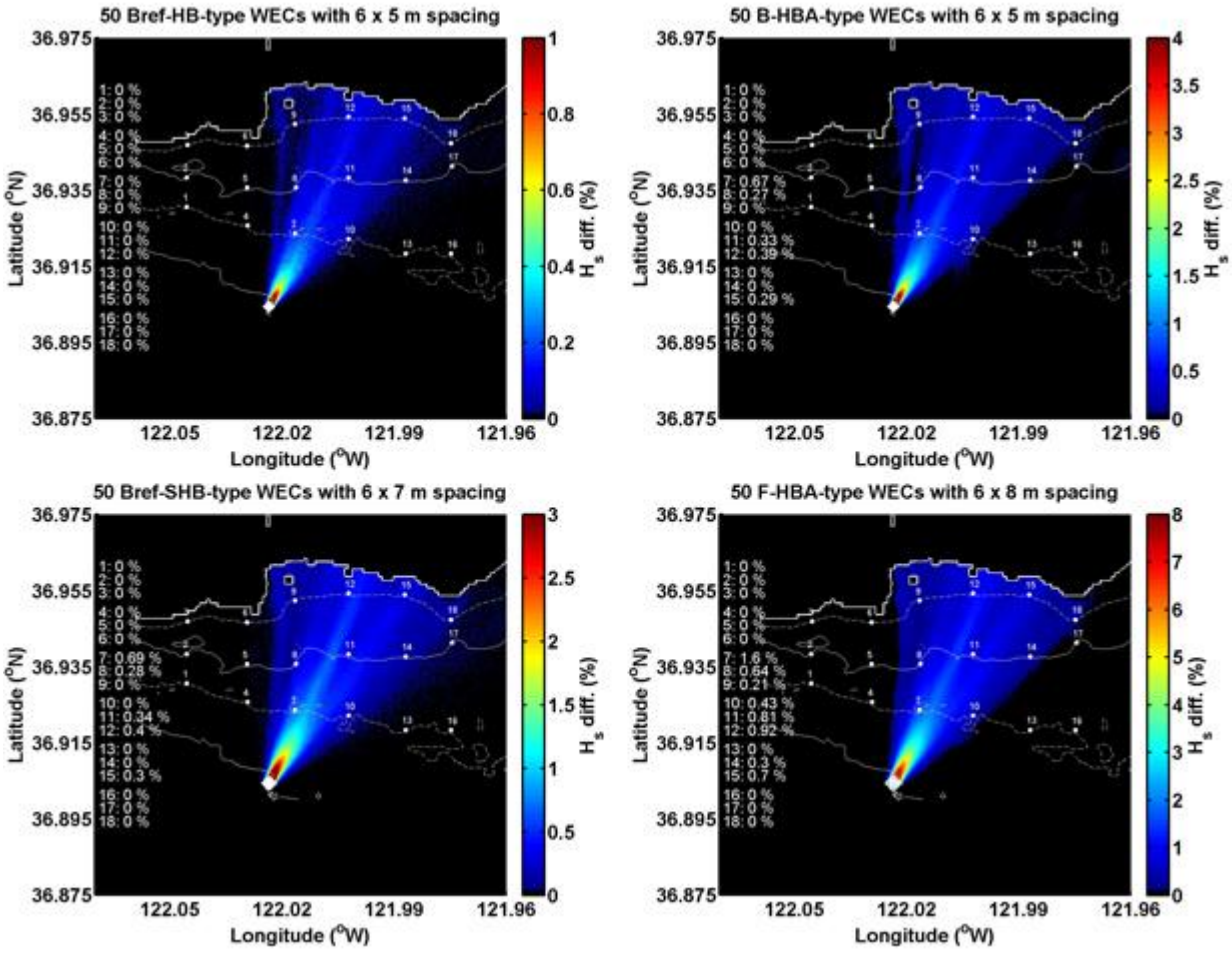

Figure 29. Significant wave height percentage decrease as a results of varying model parameters (as indicated above each panel) using SNL-SWAN Switch 1 for four of the eight WEC types. Percent differences at each of the 18 output locations are indicated on the left. Device diameters are not to scale. Note the variable scale bars.

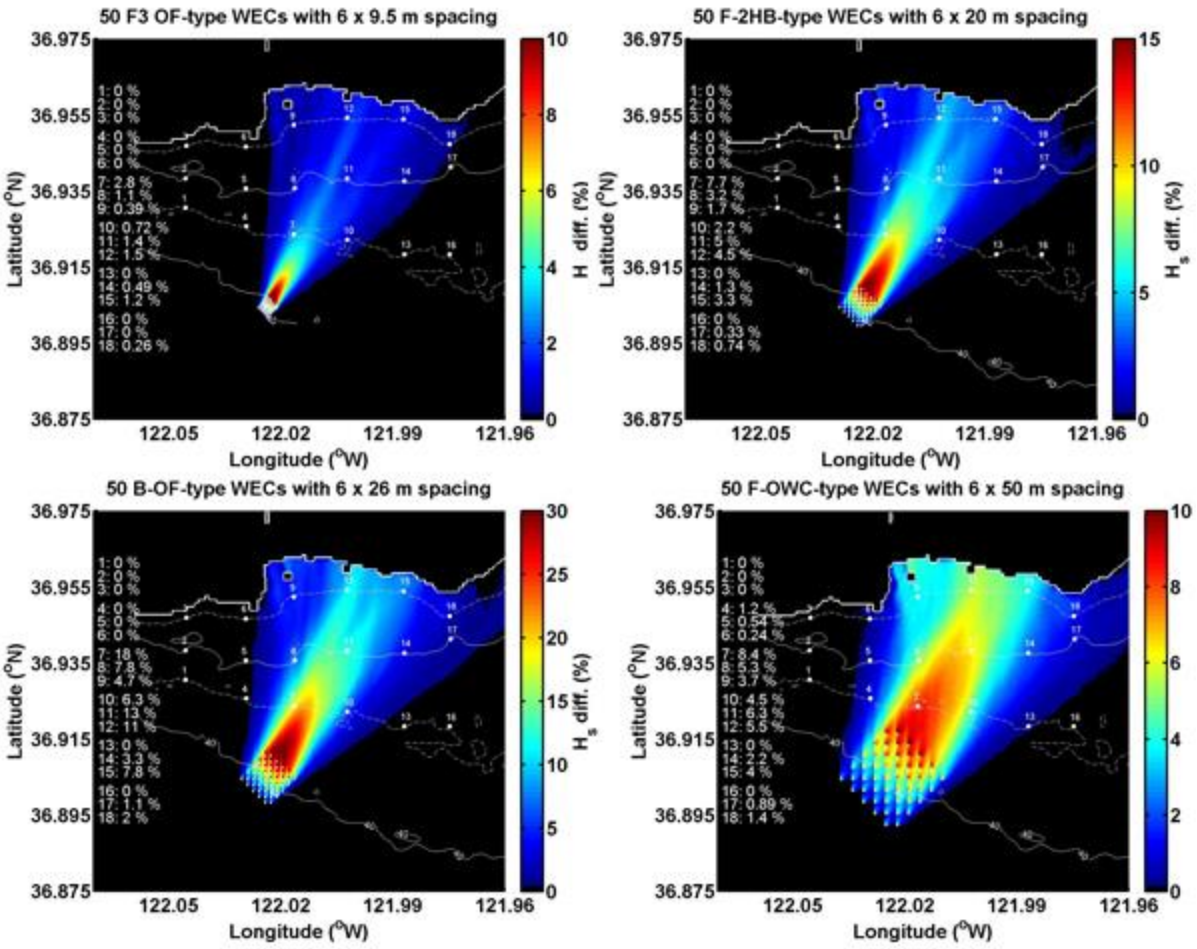

Figure 30. Same caption as for Figure 29 for the other four WEC types.

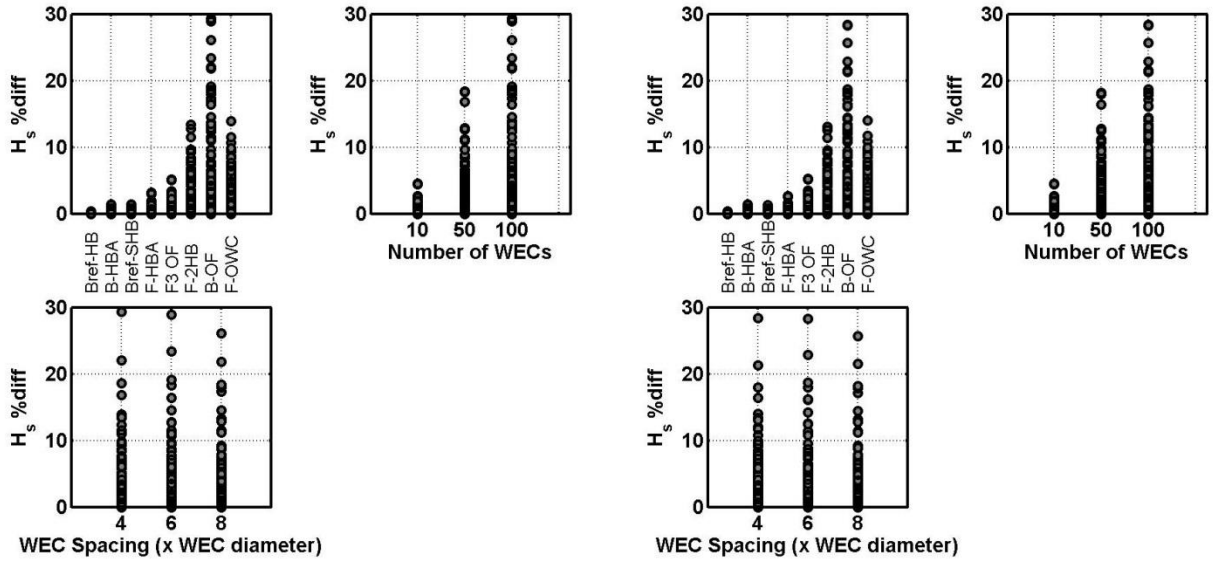

Figure 31. Variations in wave properties versus wave height reduction. The left three panels are the results from using Switch 1 and the right three panels are from Switch 2.

5.3.2 Near-bottom Orbital Velocities

As found in Section 4.3, near-bottom orbital velocities (e.g. wave-driven currents) were directly proportional to the surface wave expression (i.e. significant wave height). Decreased wave heights caused a decrease in near-bottom orbital velocities, potentially altering the ambient wave-driven currents in a near-shore environment. Consequently, the percentage differences of the near-bottom orbital velocities were essentially equivalent to those computed from the significant wave height model scenarios.

5.3.3 Peak Wave Periods

The percentage changes in peak wave periods during this study were negligible, as shown in Figure 32. The reason for this is twofold. First, within the model parameters, the frequency bin resolution may have been too large to register small changes in wave periods (small changes in frequency would not cause a change in frequency bin in model space). Second, since the model obstacles were "absorbing" the same percentage of wave energy from all wave frequencies (i.e. because the transmission coefficient is frequency-independent), there would be no change in peak wave energy; the dominant wave energy would not shift to an alternate frequency(ies). Therefore, similar to previous sensitivity analysis (Section 4.3), no change (or negligible change) was observed.

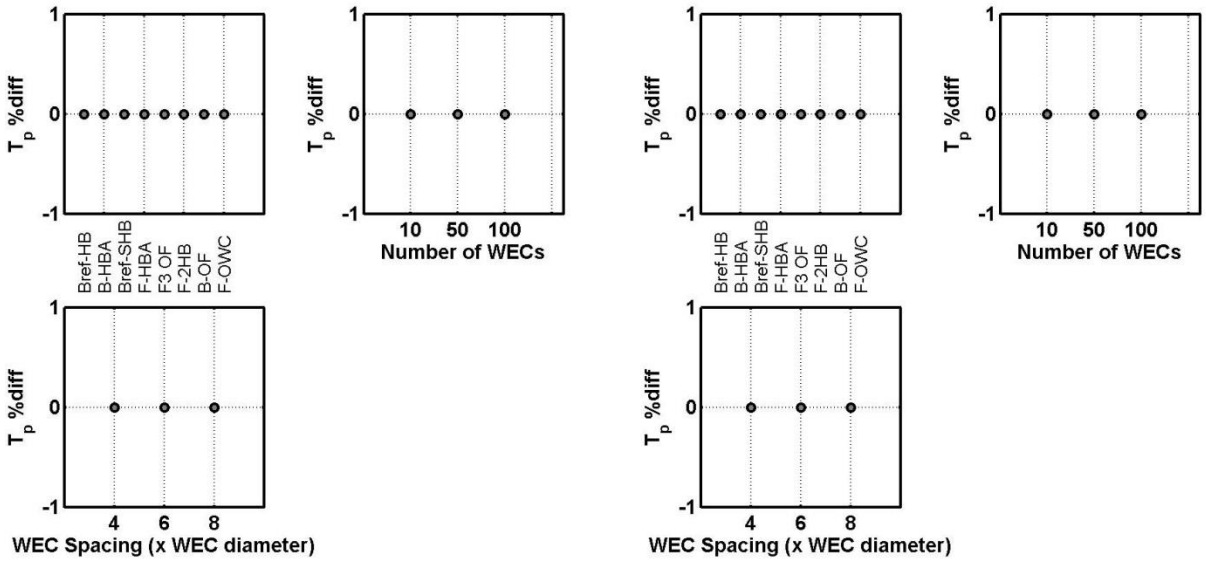

Figure 32. Variations in wave properties versus peak wave period reduction. The left three panels are the results from using Switch 1 and the right three panels are from Switch 2.

5.3.4 Mean Wave Directions

Changes in mean wave directions are illustrated in Figure 33. All percent differences translated to within ±4.5%, corresponding to ±9° change. Negative changes indicated clockwise (CW) rotation of wave direction. Positive changes indicated counter-clockwise (CCW) rotation. Rotation, when it occurred in the model, was relatively large because the directional bin spacing was equal to 9°. Any changes less than this were indeterminable by the model. Zero wave direction change was observed for modeled devices smaller than 8 m. It is thus surmised that direction changes, if any, caused by the WEC devices were less than 9°.

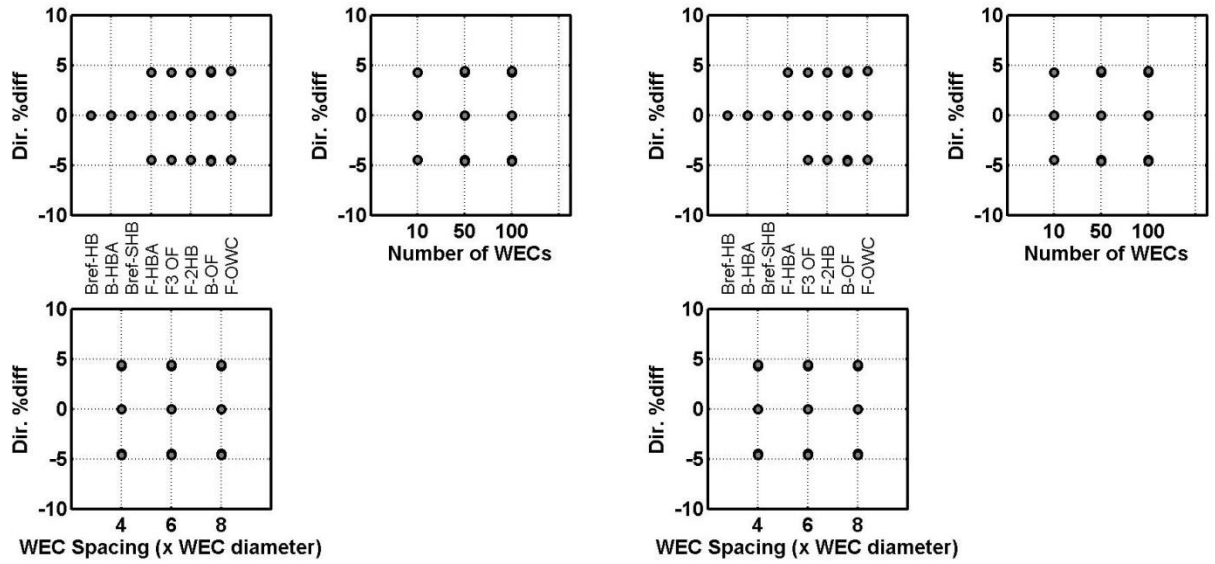

Figure 33. Variations in wave properties versus peak wave period reduction. The left three panels are the results from using Switch 1 and the right three panels are from Switch 2.

5.3.5 Results Summary

These results ultimately illustrate, that, given the present model setup, the wave heights (and associated near-bottom orbital velocities) showed decreases of up to 30% between baseline and modeled conditions for 100 devices of the B-OF buoy type. The B-OF power matrix values were largest for an incident wave height of 1.7 m. Other buoy types resulted in less than 15% differences in modeled wave height with and without obstacles, with lesser influence for buoys less than 10 m in diameter. Although the F-OWC device was the largest device modeled, its power matrix values for an incident wave height of 1.7 m were less than that of the B-OF device and hence its wave reduction potential was less. However, the F-OWC effects extended over a larger spatial extent due to its size and spacing, thereby potentially having a greater impact on the shoreline.

Wave directions and periods did not appear to be sensitive to changes in parameters. However, additional analysis is required to fully explore the model sensitivity of peak wave period and mean wave direction to the varying of the parameters.

Model output locations located to the West (output locations 1-6) showed relatively little to no change in wave heights compared to the baseline scenario. The largest wave height differences were observed downstream of the array near the array centerline (output locations 7-12), where the largest wave shadowing effects were predicted. Additional model output locations to the East (output locations 13-18) indicated relatively small changes in wave heights for buoys larger than

9 m in diameter. This all makes intuitive sense given that the modeled incident wave direction was from the southwest and these waves refracted toward the shoreline in a counter-clockwise manner.

6. SNL-SWAN SWITCH 1 AND SWITCH 2 TRANSMISSION COEFFICIENTS

The SNL-SWAN computed transmission coefficients were outputted to the model PRINT file for all sensitivity analysis model runs as summarized in Appendix B (part 2). In the interest of brevity, only model results from runs of 10 WEC devices with six diameter spacing will be discussed here. Model runs for 10 WEC devices spaced six diameters apart resulted in transmission coefficients ranging between about 0.54 and 0.99 (Figure 34). The lowest transmission coefficient values (i.e. most wave energy absorbed) were determined for the B-OF type buoy (largest power matrix values) and the highest values were found for the Bref-HB WEC type (smallest power matrix values). Correspondingly, the B-OF buoy resulted in the most reduced wave heights in the lee of the WEC array; the opposite was true for the Bref-HB device.

Because the RCW is computed as a function of wave period only and wave period did not vary over the nested model domain, transmission coefficients were consistent across all WECs in an array when Switch 2 was utilized. Switch 1 computes RCW as a function of wave height and period; therefore transmission coefficients differed slightly (less than 10%) for each WEC device in an array due to the variations in how the coefficients are interpolated. Although similar in magnitude, the transmission coefficients computed by SNL-SWAN Switch 1 and 2 differed slightly, likely due to interpolation involved in computing the RCW in Switch 2. Switch 2 transmission coefficients were not consistently higher or lower than Switch 1. The largest differences between Switch 1 and Switch 2 transmission coefficients was for the B-OF and F-HBA buoy types (differences of ~0.04 and ~0.02, respectively, compared to < 0.01 for all other devices).

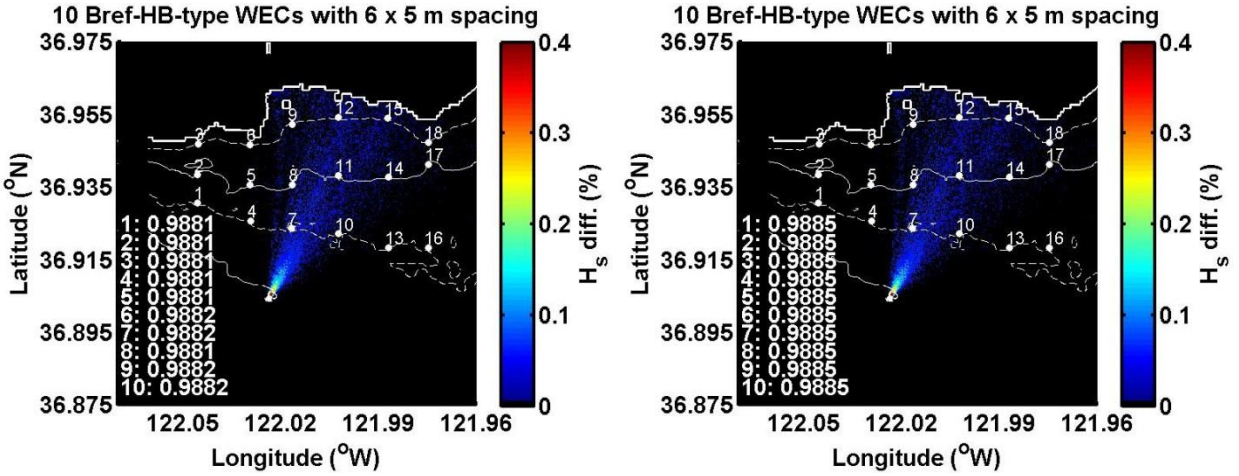

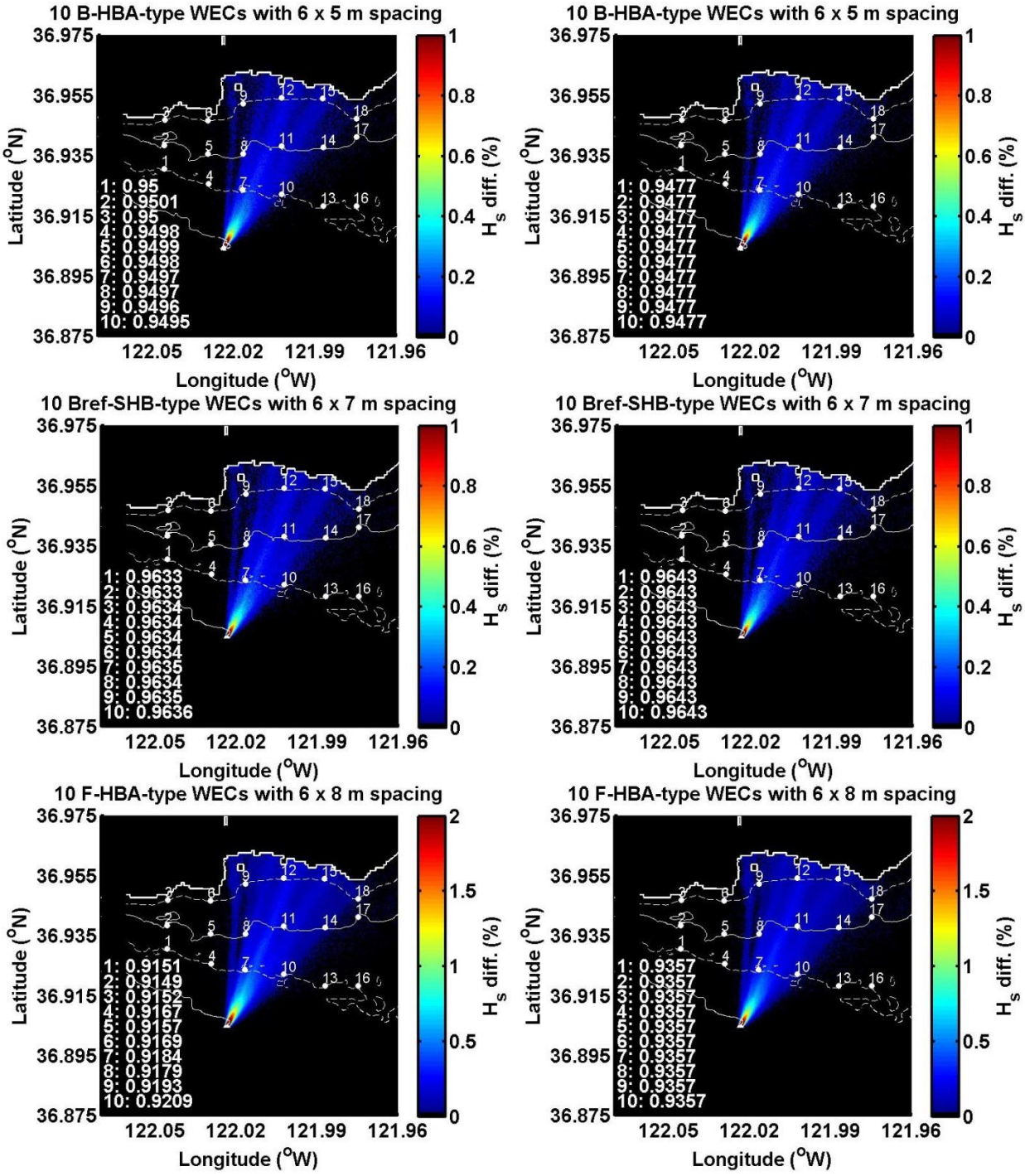
10 B-HBA-type WECs with 6 x 5 m spacing
1: 0.95
2: 0.9501
3: 0.95
4: 0.9498
5: 0.9499
6: 0.9498
7: 0.9497
8: 0.9497
9: 0.9496
10: 0.9495
10 B-HBA-type WECs with 6 x 5 m spacing
1: 0.9477
2: 0.9477
3: 0.9477
4: 0.9477
5: 0.9477
6: 0.9477
7: 0.9477
8: 0.9477
9: 0.9477
10: 0.9477
10 Bref-SHB-type WECs with 6 x 7 m spacing
1: 0.9633
2: 0.9633
3: 0.9634
4: 0.9634
5: 0.9634
6: 0.9634
7: 0.9635
8: 0.9634
9: 0.9635
10: 0.9636
10 Bref-SHB-type WECs with 6 x 7 m spacing
1: 0.9643
2: 0.9643
3: 0.9643
4: 0.9643
5: 0.9643
6: 0.9643
7: 0.9643
8: 0.9643
9: 0.9643
10: 0.9643
10 F-HBA-type WECs with 6 x 8 m spacing
1: 0.9151
2: 0.9149
3: 0.9152
4: 0.9167
5: 0.9157
6: 0.9169
7: 0.9184
8: 0.9179
9: 0.9193
10: 0.9209
10 F-HBA-type WECs with 6 x 8 m spacing
1: 0.9357
2: 0.9357
3: 0.9357
4: 0.9357
5: 0.9357
6: 0.9357
7: 0.9357
8: 0.9357
9: 0.9357
10: 0.9357
Latitude (°N)
Longitude (°W)
H_s diff. (%)

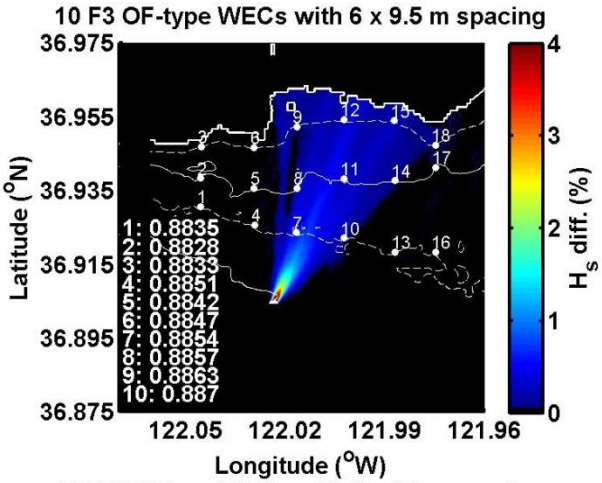
10 F3 OF-type WECs with 6 x 9.5 m spacing
1: 0.8835
2: 0.8828
3: 0.8833
4: 0.8851
5: 0.8842
6: 0.8847
7: 0.8854
8: 0.8857
9: 0.8863
10: 0.887
Latitude (°N)
Longitude (°W)
H_s diff. (%)

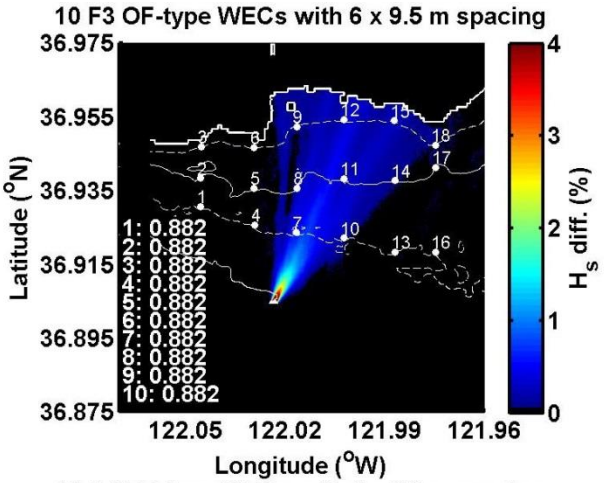
10 F3 OF-type WECs with 6 x 9.5 m spacing
1: 0.882
2: 0.882
3: 0.882
4: 0.882
5: 0.882
6: 0.882
7: 0.882
8: 0.882
9: 0.882
10: 0.882
Latitude (°N)
Longitude (°W)
H_s diff. (%)

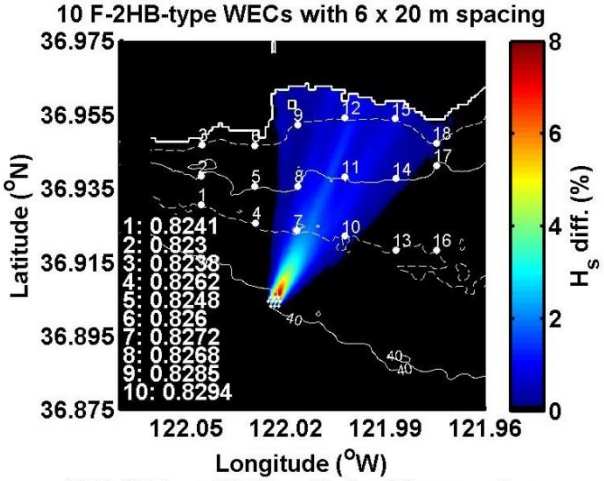
10 F-2HB-type WECs with 6 x 20 m spacing
1: 0.8241
2: 0.823
3: 0.8238
4: 0.8262
5: 0.8248
6: 0.826
7: 0.8272
8: 0.8268
9: 0.8285
10: 0.8294
Latitude (°N)
Longitude (°W)
H_s diff. (%)

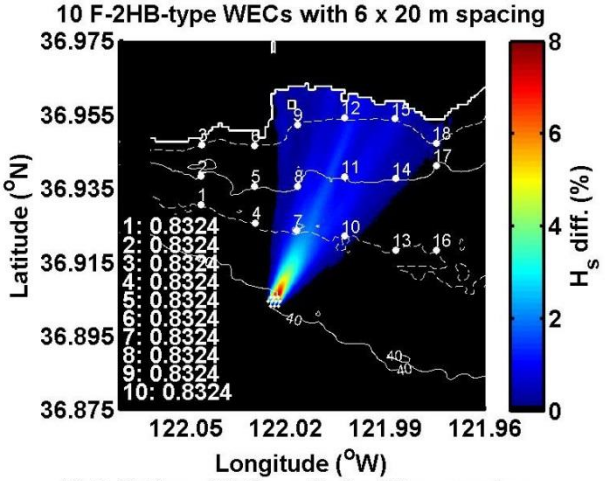
10 F-2HB-type WECs with 6 x 20 m spacing
1: 0.8324
2: 0.8324
3: 0.8324
4: 0.8324
5: 0.8324
6: 0.8324
7: 0.8324
8: 0.8324
9: 0.8324
10: 0.8324
Latitude (°N)
Longitude (°W)
H_s diff. (%)

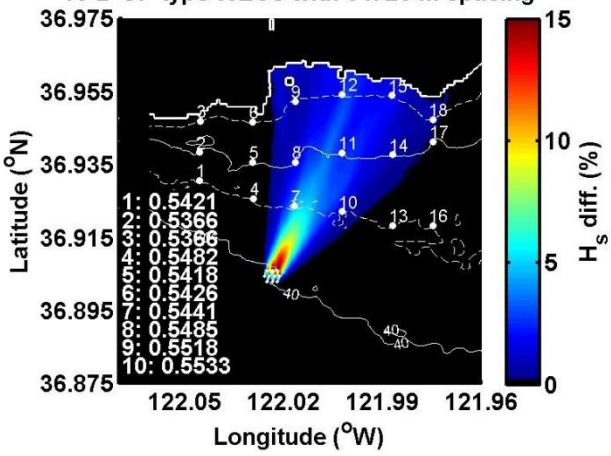
10 B-OF-type WECs with 6 x 26 m spacing
1: 0.5421
2: 0.5366
3: 0.5366
4: 0.5482
5: 0.5418
6: 0.5426
7: 0.5441
8: 0.5485
9: 0.5518
10: 0.5533
Latitude (°N)
Longitude (°W)
H_s diff. (%)

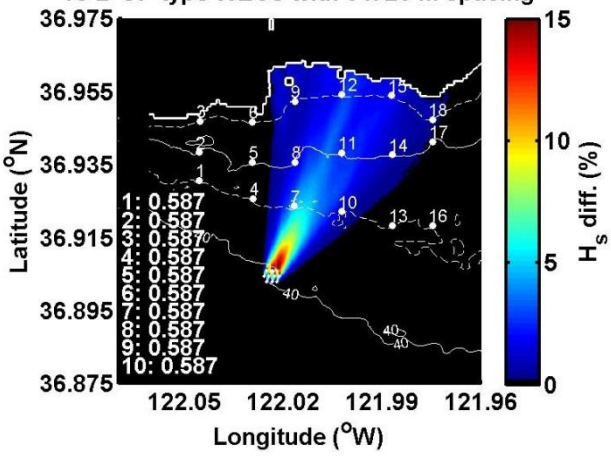
10 B-OF-type WECs with 6 x 26 m spacing
1: 0.587
2: 0.587
3: 0.587
4: 0.587
5: 0.587
6: 0.587
7: 0.587
8: 0.587
9: 0.587
10: 0.587
Latitude (°N)
Longitude (°W)
H_s diff. (%)

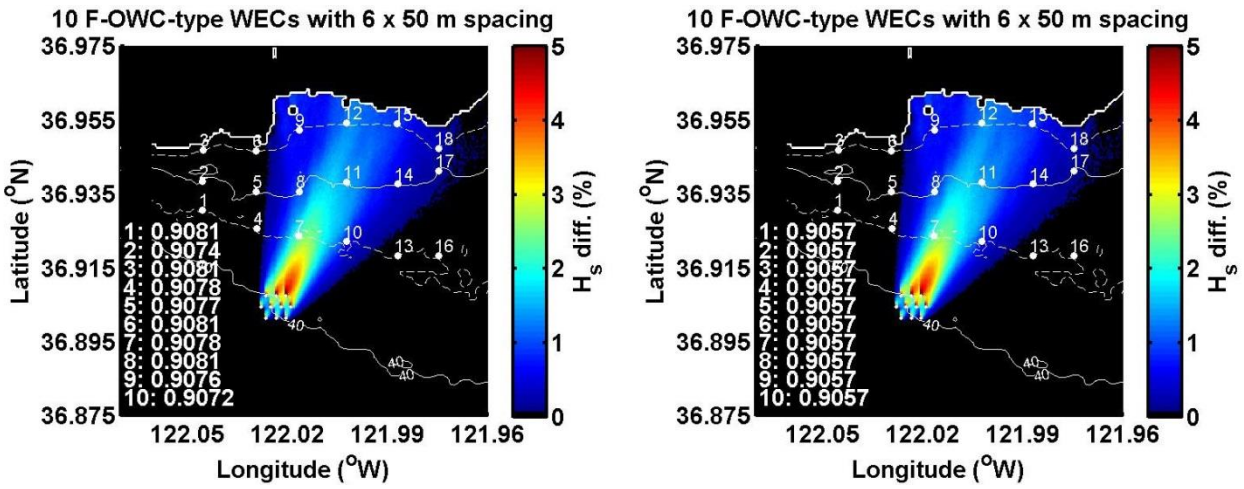

Figure 34. Significant wave height percentage decrease using SNL-SWAN Switch 1 (left) and Switch 2 (right) for eight different WEC device types. SNL-SWAN computed transmission coefficients for each of the 10 WECs in the WEC array are indicated on the left. Note the different color bar scales.

7. CONCLUSIONS

The presence of WEC arrays have the potential to alter wave propagation patterns significantly and affect coastal circulation patterns, sediment transport patterns, and alter ecosystem processes. To help accelerate deployment of environmentally friendly WEC arrays, predictive modeling tools must be developed to accurately represent WEC induced changes in wave propagation and evaluate the potential for environmental impact. The present study utilized a modified version (SNL-SWAN) of an industry standard wave modeling tool, SWAN, to examine potential WEC array deployment scenarios at a site on the California coast and investigate model sensitivity so that the model can be effectively and confidently used in environmental studies. This analysis built upon a previous sensitivity analysis in which SWAN model parameters were varied to examine their effect on model results (Chang et al., 2014)

In the present study, the modified SWAN wave model, SNL- SWAN, was evaluated against the native SWAN code and used to investigate the effects of different WEC devices on near-shore wave propagation. SNL-SWAN model parameters were optimized in terms of the following model parameters: directional spread, direction resolution, and diffraction. Two different SNL-SWAN sensitivity analysis studies were performed to examine the effects of model and WEC variations (incident wave height, period, frequency distribution spread, and directional distribution spread; and WEC device type and size, number of WEC devices in an array, and the spacing of the WEC devices within the array) on near-field and far-field wave conditions in the lee of the WEC devices to better understand the functionality of SNL- SWAN and identify code concerns early in the development process.

The sensitivity studies illustrated that wave direction and WEC device type were most sensitive to the variation in the parameters examined in this study. Wave heights were minimally affected by wave parameter variation. Locations in the lee centerline of the arrays in each modeled scenario showed the largest potential changes in wave height (and near-bottom orbital velocity) compared to those at the eastern and western fringes of the shadow zone.

Significant wave height was most sensitive to variations in WEC device type and size and the number of WEC devices in an array. This makes intuitive sense as each device has a device-specific power matrix and associated RCW and the power matrix values are highly variable. Locations in the lee centerline of the arrays in each modeled scenario showed the largest potential changes in wave height (and near-bottom orbital velocity), followed by those on edge of the shadow in the direction of wave propagation. In these cases the shadow was skewed to the east as expected for a wave with a westerly component.

It is important to utilize ongoing laboratory studies and future field tests to determine the most appropriate power matrix values for a particular WEC device and configuration. Until power matrix values can be accurately determined or further WEC ‘friendly’ model enhancements are validated, this study shows that environmental assessments of WEC devices should focus on evaluating a range of WEC characteristics in order to determine the limits of the potential environmental effects resulting from the presence of a WEC array.

In summary, the present study developed a baseline model understanding while investigating the effects of a range of WEC devices. The sensitivity, optimization, and behavior of the model for various WEC devices provided the basis for a solid model understanding giving the confidence necessary for future WEC evaluations.

8. REFERENCES

1. Babarit, A., J. Hals, M.J. Muliawan, A. Kurniawan, T. Moan, and J. Krokstad, 2012, Numerical benchmarking study of a selection of wave energy converters, Renewable Energy, 41, 44-63.

2. Booij, N., L.H. Holthuijsen, and R.C. Ris, 1996, The SWAN wave model for shallow water, Proc. 25th Int. Conf. Coastal Engng., Orlando, USA, Vol. 1, pp. 668-676.

3. Chang, G and C. Jones, D. Hansen, M. Twardowski and A. Barnard, 2010, Prediction of Optical Variability in Dynamic Near-shore Environments: Task Completion Report #3 – Numerical Modeling and Verification. 28 pp.

4. Chang, G., J. Magalen, C. Jones, and J. Roberts, 2014, Investigation of Wave Energy Converter Effects on Wave Fields: A Modeling Sensitivity Study in Monterey Bay, CA, Tech. Rep. SAND2014-16840, Sandia National Laboratories, Albuquerque, NM, 65 pp.

5. Delft University of Technology (2011) SWAN User Manual, Delft, The Netherlands, 129 pp.

APPENDIX A: SNL-SWAN SENSITIVITY ANALYSIS MODELED SCENARIOS – PART 1

Run	Input Hs (m)	Input Tp (s)	Input MWD (deg)	Reflection Coefficient	Gamma – Freq Spreading	M – Dir Spreading (power)	WEC Device Type	# WEC Devices	Array Depth (m)
1	1.7	12.5	205	0	1	2	B-OF	10	40
2	1.7	12.5	205	0	1	10	B-OF	10	40
3	1.7	12.5	205	0	1	25	B-OF	10	40
4	1.7	12.5	205	0	3.3	2	B-OF	10	40
5	1.7	12.5	205	0	3.3	10	B-OF	10	40
6	1.7	12.5	205	0	3.3	25	B-OF	10	40
7	1.7	12.5	205	0	10	2	B-OF	10	40
8	1.7	12.5	205	0	10	10	B-OF	10	40
9	1.7	12.5	205	0	10	25	B-OF	10	40
10	1.7	16	205	0	1	2	B-OF	10	40
11	1.7	16	205	0	1	10	B-OF	10	40
12	1.7	16	205	0	1	25	B-OF	10	40
13	1.7	16	205	0	3.3	2	B-OF	10	40
14	1.7	16	205	0	3.3	10	B-OF	10	40
15	1.7	16	205	0	3.3	25	B-OF	10	40
16	1.7	16	205	0	10	2	B-OF	10	40
17	1.7	16	205	0	10	10	B-OF	10	40
18	1.7	16	205	0	10	25	B-OF	10	40
19	3.5	12.5	205	0	1	2	B-OF	10	40
20	3.5	12.5	205	0	1	10	B-OF	10	40
21	3.5	12.5	205	0	1	25	B-OF	10	40
22	3.5	12.5	205	0	3.3	2	B-OF	10	40
23	3.5	12.5	205	0	3.3	10	B-OF	10	40
24	3.5	12.5	205	0	3.3	25	B-OF	10	40
25	3.5	12.5	205	0	10	2	B-OF	10	40
26	3.5	12.5	205	0	10	10	B-OF	10	40
27	3.5	12.5	205	0	10	25	B-OF	10	40
28	3.5	16	205	0	1	2	B-OF	10	40
29	3.5	16	205	0	1	10	B-OF	10	40
30	3.5	16	205	0	1	25	B-OF	10	40
31	3.5	16	205	0	3.3	2	B-OF	10	40
32	3.5	16	205	0	3.3	10	B-OF	10	40
33	3.5	16	205	0	3.3	25	B-OF	10	40
34	3.5	16	205	0	10	2	B-OF	10	40
35	3.5	16	205	0	10	10	B-OF	10	40
36	3.5	16	205	0	10	25	B-OF	10	40
37	1.7	12.5	205	0	1	2	F-2HB	10	40
38	1.7	12.5	205	0	1	10	F-2HB	10	40
39	1.7	12.5	205	0	1	25	F-2HB	10	40
40	1.7	12.5	205	0	3.3	2	F-2HB	10	40
41	1.7	12.5	205	0	3.3	10	F-2HB	10	40

42	1.7	12.5	205	0	3.3	25	F-2HB	10	40
43	1.7	12.5	205	0	10	2	F-2HB	10	40
44	1.7	12.5	205	0	10	10	F-2HB	10	40
45	1.7	12.5	205	0	10	25	F-2HB	10	40
46	1.7	16	205	0	1	2	F-2HB	10	40
47	1.7	16	205	0	1	10	F-2HB	10	40
48	1.7	16	205	0	1	25	F-2HB	10	40
49	1.7	16	205	0	3.3	2	F-2HB	10	40
50	1.7	16	205	0	3.3	10	F-2HB	10	40
51	1.7	16	205	0	3.3	25	F-2HB	10	40
52	1.7	16	205	0	10	2	F-2HB	10	40
53	1.7	16	205	0	10	10	F-2HB	10	40
54	1.7	16	205	0	10	25	F-2HB	10	40
55	3.5	12.5	205	0	1	2	F-2HB	10	40
56	3.5	12.5	205	0	1	10	F-2HB	10	40
57	3.5	12.5	205	0	1	25	F-2HB	10	40
58	3.5	12.5	205	0	3.3	2	F-2HB	10	40
59	3.5	12.5	205	0	3.3	10	F-2HB	10	40
60	3.5	12.5	205	0	3.3	25	F-2HB	10	40
61	3.5	12.5	205	0	10	2	F-2HB	10	40
62	3.5	12.5	205	0	10	10	F-2HB	10	40
63	3.5	12.5	205	0	10	25	F-2HB	10	40
64	3.5	16	205	0	1	2	F-2HB	10	40
65	3.5	16	205	0	1	10	F-2HB	10	40
66	3.5	16	205	0	1	25	F-2HB	10	40
67	3.5	16	205	0	3.3	2	F-2HB	10	40
68	3.5	16	205	0	3.3	10	F-2HB	10	40
69	3.5	16	205	0	3.3	25	F-2HB	10	40
70	3.5	16	205	0	10	2	F-2HB	10	40
71	3.5	16	205	0	10	10	F-2HB	10	40
72	3.5	16	205	0	10	25	F-2HB	10	40
73	1.7	12.5	205	0	1	2	F-OWC	10	40
74	1.7	12.5	205	0	1	10	F-OWC	10	40
75	1.7	12.5	205	0	1	25	F-OWC	10	40
76	1.7	12.5	205	0	3.3	2	F-OWC	10	40
77	1.7	12.5	205	0	3.3	10	F-OWC	10	40
78	1.7	12.5	205	0	3.3	25	F-OWC	10	40
79	1.7	12.5	205	0	10	2	F-OWC	10	40
80	1.7	12.5	205	0	10	10	F-OWC	10	40
81	1.7	12.5	205	0	10	25	F-OWC	10	40

82	1.7	16	205	0	1	2	F-OWC	10	40
83	1.7	16	205	0	1	10	F-OWC	10	40
84	1.7	16	205	0	1	25	F-OWC	10	40
85	1.7	16	205	0	3.3	2	F-OWC	10	40
86	1.7	16	205	0	3.3	10	F-OWC	10	40
87	1.7	16	205	0	3.3	25	F-OWC	10	40
88	1.7	16	205	0	10	2	F-OWC	10	40
89	1.7	16	205	0	10	10	F-OWC	10	40
90	1.7	16	205	0	10	25	F-OWC	10	40
91	3.5	12.5	205	0	1	2	F-OWC	10	40
92	3.5	12.5	205	0	1	10	F-OWC	10	40
93	3.5	12.5	205	0	1	25	F-OWC	10	40
94	3.5	12.5	205	0	3.3	2	F-OWC	10	40
95	3.5	12.5	205	0	3.3	10	F-OWC	10	40
96	3.5	12.5	205	0	3.3	25	F-OWC	10	40
97	3.5	12.5	205	0	10	2	F-OWC	10	40
98	3.5	12.5	205	0	10	10	F-OWC	10	40
99	3.5	12.5	205	0	10	25	F-OWC	10	40
100	3.5	16	205	0	1	2	F-OWC	10	40
101	3.5	16	205	0	1	10	F-OWC	10	40
102	3.5	16	205	0	1	25	F-OWC	10	40
103	3.5	16	205	0	3.3	2	F-OWC	10	40
104	3.5	16	205	0	3.3	10	F-OWC	10	40
105	3.5	16	205	0	3.3	25	F-OWC	10	40
106	3.5	16	205	0	10	2	F-OWC	10	40

107	3.5	16	205	0	10	10	F-OWC	10	40
108	3.5	16	205	0	10	25	F-OWC	10	40

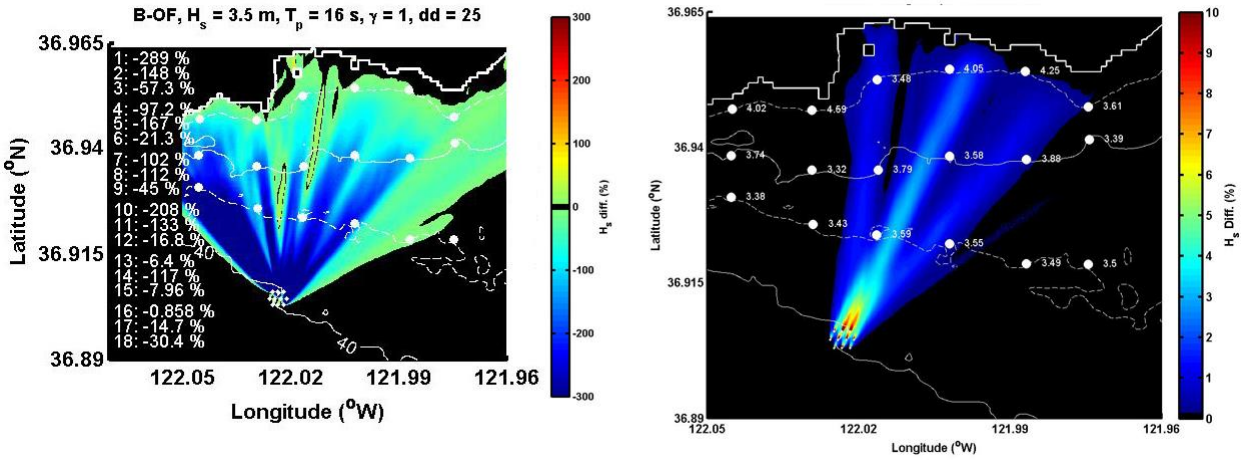

Figure A 1. Significant wave height percentage decrease using SNL-SWAN Switch 2 illustrating the error in the SNL-SWAN code in passing variables from the model to the output PRINT file (Left) and the results after the code was debugged and fixed (Right).

APPENDIX B: SNL-SWAN SENSITIVITY ANALYSIS MODELED SCENARIOS – PART 2

Run	Input Hs (m)	Input Tp (s)	Input MWD (deg)	Gamma – Freq Spread	M – Dir Spread (power)	Array Depth (m)	WEC Device Type	# WEC Devices	WEC Spacing
1	1.7	12.5	205	3.3	25	40	Bref-HB	10	4
2	1.7	12.5	205	3.3	25	40	Bref-HB	10	6
3	1.7	12.5	205	3.3	25	40	Bref-HB	10	8
4	1.7	12.5	205	3.3	25	40	Bref-HB	50	4
5	1.7	12.5	205	3.3	25	40	Bref-HB	50	6
6	1.7	12.5	205	3.3	25	40	Bref-HB	50	8
7	1.7	12.5	205	3.3	25	40	Bref-HB	100	4
8	1.7	12.5	205	3.3	25	40	Bref-HB	100	6
9	1.7	12.5	205	3.3	25	40	Bref-HB	100	8
10	1.7	12.5	205	3.3	25	40	B-HBA	10	4
11	1.7	12.5	205	3.3	25	40	B-HBA	10	6
12	1.7	12.5	205	3.3	25	40	B-HBA	10	8
13	1.7	12.5	205	3.3	25	40	B-HBA	50	4
14	1.7	12.5	205	3.3	25	40	B-HBA	50	6
15	1.7	12.5	205	3.3	25	40	B-HBA	50	8
16	1.7	12.5	205	3.3	25	40	B-HBA	100	4
17	1.7	12.5	205	3.3	25	40	B-HBA	100	6
18	1.7	12.5	205	3.3	25	40	B-HBA	100	8
19	1.7	12.5	205	3.3	25	40	Bref-SHB	10	4
20	1.7	12.5	205	3.3	25	40	Bref-SHB	10	6
21	1.7	12.5	205	3.3	25	40	Bref-SHB	10	8
22	1.7	12.5	205	3.3	25	40	Bref-SHB	50	4
23	1.7	12.5	205	3.3	25	40	Bref-SHB	50	6
24	1.7	12.5	205	3.3	25	40	Bref-SHB	50	8
25	1.7	12.5	205	3.3	25	40	Bref-SHB	100	4
26	1.7	12.5	205	3.3	25	40	Bref-SHB	100	6
27	1.7	12.5	205	3.3	25	40	Bref-SHB	100	8
28	1.7	12.5	205	3.3	25	40	F-HBA	10	4
29	1.7	12.5	205	3.3	25	40	F-HBA	10	6
30	1.7	12.5	205	3.3	25	40	F-HBA	10	8
31	1.7	12.5	205	3.3	25	40	F-HBA	50	4
32	1.7	12.5	205	3.3	25	40	F-HBA	50	6
33	1.7	12.5	205	3.3	25	40	F-HBA	50	8
34	1.7	12.5	205	3.3	25	40	F-HBA	100	4
35	1.7	12.5	205	3.3	25	40	F-HBA	100	6
36	1.7	12.5	205	3.3	25	40	F-HBA	100	8
37	1.7	12.5	205	3.3	25	40	F3 OF	10	4
38	1.7	12.5	205	3.3	25	40	F3 OF	10	6
39	1.7	12.5	205	3.3	25	40	F3 OF	10	8
40	1.7	12.5	205	3.3	25	40	F3 OF	50	4
41	1.7	12.5	205	3.3	25	40	F3 OF	50	6
42	1.7	12.5	205	3.3	25	40	F3 OF	50	8

43	1.7	12.5	205	3.3	25	40	F3 OF	100	4
44	1.7	12.5	205	3.3	25	40	F3 OF	100	6
45	1.7	12.5	205	3.3	25	40	F3 OF	100	8
46	1.7	12.5	205	3.3	25	40	F-2HB	10	4
47	1.7	12.5	205	3.3	25	40	F-2HB	10	6
48	1.7	12.5	205	3.3	25	40	F-2HB	10	8
49	1.7	12.5	205	3.3	25	40	F-2HB	50	4
50	1.7	12.5	205	3.3	25	40	F-2HB	50	6
51	1.7	12.5	205	3.3	25	40	F-2HB	50	8
52	1.7	12.5	205	3.3	25	40	F-2HB	100	4
53	1.7	12.5	205	3.3	25	40	F-2HB	100	6
54	1.7	12.5	205	3.3	25	40	F-2HB	100	8
55	1.7	12.5	205	3.3	25	40	B-OF	10	4
56	1.7	12.5	205	3.3	25	40	B-OF	10	6
57	1.7	12.5	205	3.3	25	40	B-OF	10	8
58	1.7	12.5	205	3.3	25	40	B-OF	50	4
59	1.7	12.5	205	3.3	25	40	B-OF	50	6
60	1.7	12.5	205	3.3	25	40	B-OF	50	8
61	1.7	12.5	205	3.3	25	40	B-OF	100	4
62	1.7	12.5	205	3.3	25	40	B-OF	100	6
63	1.7	12.5	205	3.3	25	40	B-OF	100	8
64	1.7	12.5	205	3.3	25	40	F-OWC	10	4
65	1.7	12.5	205	3.3	25	40	F-OWC	10	6
66	1.7	12.5	205	3.3	25	40	F-OWC	10	8
67	1.7	12.5	205	3.3	25	40	F-OWC	50	4
68	1.7	12.5	205	3.3	25	40	F-OWC	50	6
69	1.7	12.5	205	3.3	25	40	F-OWC	50	8
70	1.7	12.5	205	3.3	25	40	F-OWC	100	4
71	1.7	12.5	205	3.3	25	40	F-OWC	100	6
72	1.7	12.5	205	3.3	25	40	F-OWC	100	8

DISTRIBUTION

4 Lawrence Livermore National Laboratory
Attn: N. Dunipace (1)
P.O. Box 808, MS L-795
Livermore, CA 94551-0808

1	MS0899	Technical Library	9536 (electronic copy)


Sandia National Laboratories